Deep-Sea Research II 55 (2008) 1398–1411

Contents lists available at ScienceDirect

Deep-Sea Research II

journal homepage: www.elsevier.com/locate/dsr2

Nitrogen dynamics within a wind-driven eddy

Claire Mahaffey [a,*], Claudia R. Benitez-Nelson [b,1], Robert R. Bidigare [a,2], Yoshimi Rii [a,3], David M. Karl [a,4]

[a] Department of Oceanography, University of Hawaii, Honolulu, HI 96822, USA
[b] Department of Geological Sciences and Marine Science Program, University of South Carolina, Columbia, SC 29208, USA

ARTICLE INFO

Article history:
Accepted 5 February 2008
Available online 21 May 2008

Keywords:
Nitrogen cycle
Nitrogen isotopes
Cyclonic eddies
Export production
North Pacific Ocean

ABSTRACT

Wind-driven cyclonic eddies are hypothesized to relieve nutrient stress and enhance primary production by the upward displacement of nutrient-rich deep waters into the euphotic zone. In this study, we measured nitrate (NO_3^-), particulate carbon (PC), particulate nitrogen (PN), their stable isotope compositions (δ^{15}N-NO_3^-, δ^{13}C-PC and δ^{15}N-PN, respectively), and dissolved organic nitrogen (DON) within Cyclone *Opal*, a mature wind-driven eddy generated in the lee of the Hawaiian Islands. Sampling occurred in March 2005 as part of the multi-disciplinary E-Flux study, approximately 4–6 weeks after eddy formation. Integrated NO_3^- concentrations above 110 m were 4.8 times greater inside the eddy (85.8 ± 6.4 mmol N m^{-2}) compared to the surrounding water column (17.8 ± 7.8 mmol N m^{-2}). Using N-isotope derived estimates of NO_3^- assimilation, we estimated that 213 ± 59 mmol m^{-2} of NO_3^- was initially injected into the upper 110 m Cyclone *Opal* formation, implying that NO_3^- was assimilated at a rate of 3.75 ± 0.5 mmol N m^{-2} d^{-1}. This injected NO_3^- supported $68 \pm 19\%$ and $66 \pm 9\%$ of the phytoplankton N demand and export production, respectively. N isotope data suggest that $32 \pm 6\%$ of the initial NO_3^- remained unassimilated. Self-shading, inefficiency in the transfer of N from dissolved to particulate export, or depletion of a specific nutrient other than N may have led to a lack of complete NO_3^- assimilation. Using a salt budget approach, we estimate that dissolved organic nitrogen (DON) concentrations increased from eddy formation (3.8 ± 0.4 mmol N m^{-2}) to the time of sampling (4.0 ± 0.09 mmol N m^{-2}), implying that DON accumulated at rate of 0.83 ± 1.3 mmol N m^{-2} d^{-1}, and accounted for $22 \pm 15\%$ of the injected NO_3^-. Interestingly, no significant increase in suspended PN and PC, or export production was observed inside Cyclone *Opal* relative to the surrounding water column. A simple N budget shows that if $22 \pm 15\%$ of the injected NO_3^- was shunted into the DON pool, and $32 \pm 6\%$ is unassimilated, then $46 \pm 16\%$ of the injected NO_3^- remains undocumented. Alternative loss processes within the eddy include lateral exchange of injected NO_3^- along isopycnal surfaces, remineralization of PN at depth, as well as microzooplankton grazing. A 9-day time series within Cyclone *Opal* revealed a temporal depletion in δ^{15}N-PN, implying a rapid change in the N source. A change in NO_3^- assimilation, or a shift from NO_3^- fueled growth to assimilation of a ^{15}N-deplete N source, may be responsible for such observations.

1. Introduction

Nitrogen (N) is an essential element for the growth of all organisms. In the oligotrophic open ocean, the upward diffusive flux and coupled autotrophic assimilation of nitrate (NO_3^-), termed "new" production (Dugdale and Goering, 1967), are typically low due to thermal stratification of the water column. Thus, phytoplankton production is mostly sustained by "regenerated" nutrients, such as ammonium (NH_4^+) and dissolved organic nitrogen (DON) (Dugdale and Goering, 1967), or by other N sources, including biological fixation of dinitrogen (N_2) and wet and dry deposition of atmospheric fixed N (Lipschultz et al., 2002).

Upwelling may temporarily alleviate NO_3^- limitation in the surface ocean due to the uplift of nutrient-rich waters into the sunlit layer at the surface. This process may be driven by a number of physical mechanisms including fronts (Mahadevan and Archer, 2000), instability waves (Strutton et al., 2001), Rossby waves (Uz et al., 2001; Siegel, 2001), and cold-core or cyclonic eddies (Falkowski et al., 1991; McGillicuddy and Robinson, 1997;

* Corresponding author. Present address: Department of Earth and Ocean Sciences, University of Liverpool, Liverpool L69 4GP, UK. Tel.: +44 151 794 4090; fax: +44 151 794 5196.
E-mail addresses: mahaffey@liv.ac.uk (C. Mahaffey), cbnelson@geol.sc.edu (C.R. Benitez-Nelson), bidigare@hawaii.edu (R.R. Bidigare), shimi@hawaii.edu (Y. Rii), dkarl@hawaii.edu (D.M. Karl).
[1] Tel.: +1 803 777 0018; fax: +1 803 777 6610.
[2] Tel.: +1 808 956 7941; fax: +1 808 956 9516.
[3] Tel.: +1 808 956 7632; fax: +1 808 956 9516.
[4] Tel.: +1 808 956 8964; fax: +1 808 956 5059.

0967-0645/$ - see front matter © 2008 Elsevier Ltd. All rights reserved.
doi:10.1016/j.dsr2.2008.02.004

McGillicuddy et al., 1998, 1999). Several studies have observed a 3–9-fold increase in euphotic zone NO_3^- concentrations due to the passage of cyclonic eddies (Allen et al., 1996; Seki et al., 2001; Bidigare et al., 2003) and Rossby waves (Sakamoto et al., 2004). These nutrient increases further resulted in substantial enhancements in primary production and plankton biomass as well as a shift in plankton community structure (Bidigare et al., 2003; Sweeney et al., 2003; Vaillancourt et al., 2003; Falkowski et al., 1991; Allen et al., 1996). Therefore, cyclonic eddies also are hypothesized to increase new production and the export of carbon (C), N and other essential bio-elements from the surface to the deep ocean (McGillicuddy et al., 2007), however few studies have been able to quantify their impact directly.

The waters surrounding the Hawaiian archipelago in the North Pacific Ocean are largely oligotrophic. Trade winds funnel through the subaerial topography of the Hawaiian Islands, specifically Maui and Hawaii, and induce the formation of cold-core cyclonic eddies on a semi-regular basis (Patzert, 1969; Lumpkin, 1998; Chavanne et al., 2002). E-Flux was a multidisciplinary effort to understand the interaction between mesoscale eddy physics and biogeochemistry and presented an ideal opportunity to study N-biogeochemistry; the distribution of dissolved and particulate inorganic and organic N. Stable N isotopes of dissolved and particulate N were further used to understand better N assimilation and the ultimate fate of the upwelled NO_3^-.

Nitrogen exists in nature as two stable isotopes, ^{14}N (99.63%) and ^{15}N (0.37%), with the ratio of ^{14}N and ^{15}N in a sample relative to atmospheric N_2 expressed in the δ-notation (see Section 2) with units in per mil (‰) (Wada and Hattori, 1976; Wada, 1980). Two factors influence the $\delta^{15}N$ of phytoplankton in the surface ocean: (1) the $\delta^{15}N$ of the N source and (2) the biotic and abiotic discriminations between ^{15}N and ^{14}N during the transformation of N from one form to another (Mariotti et al., 1981; Sigman and Casciotti, 2001). Both N_2 fixation ($\delta^{15}N$ of dissolved N_2 ~0.6‰) and assimilation of regenerated NH_4^+ ($\delta^{15}N\text{-}NH_4^+ < 1.0$‰) result in ^{15}N-depleted plankton (<2‰, Wada and Hattori, 1976; Saino and Hattori, 1987; Checkley and Miller, 1989; Carpenter et al., 1997). The $\delta^{15}N$ of the bulk material, high molecular weight DON fraction, proteins (Knapp et al., 2005; Meador et al., 2007) and atmospheric NO_3^- (Hastings et al., 2003) are partially characterized, but their assimilation by microorganisms is poorly constrained.

Eddy-induced uplift and autotrophic assimilation of NO_3^- has the potential to alter $\delta^{15}N$ signatures in the surface ocean (Waser et al., 2000; Mahaffey et al., 2004), and will depend upon the value of $\delta^{15}N\text{-}NO_3^-$ upwelled from below, the rate of NO_3^- supply relative to assimilation, and export of ^{15}N out of the euphotic zone. In a closed system, following a single pulsed input of NO_3^-, the $\delta^{15}N$-PN will be close to the $\delta^{15}N$ of the initial NO_3^- source and will conform to Rayleigh fractionation kinetics (Mariotti et al., 1981; Altabet, 1996; Waser et al., 2000; Sigman and Casciotti, 2001). In an open system, where the rate of supply is greater than the rate of assimilation, the $\delta^{15}N$-PN will be characterized by steady-state fractionation kinetics, such that the $\delta^{15}N$-PN is equal to the $\delta^{15}N$-source minus the fractionation factor of that specific substrate (Mariotti et al., 1981; Altabet, 1996; Waser et al., 2000; Sigman and Casciotti, 2001).

The carbon isotopic composition of phytoplankton (ratio between ^{12}C and ^{13}C, expressed as $\delta^{13}C$-PC) reflects fractionation processes that occur during photosynthesis. The degree of discrimination is affected by several processes, including carbon dioxide (CO_2) concentration, cell size, growth rate and CO_2 supply versus demand (Rau et al., 1992; Kennedy and Robertson, 1995; Popp et al., 1999). Typical oceanic $\delta^{13}C$-PC values are approximately −22‰, with ^{13}C-enriched values being associated with CO_2 drawdown (Rau et al., 1992) and high growth rates (Laws et al., 1995), as well as variations in sea-surface temperature (Kennedy and Robertson, 1995).

In this study, we present results from the E-Flux III cruise in March 2005 that sampled a large mesoscale cold-core cyclonic eddy, Cyclone *Opal* (Benitez-Nelson et al., 2007; Dickey et al., 2008). Using seawater and particulate samples collected inside and outside the mesoscale feature, we compare the vertical structure of NO_3^-, DON, particulate biomass (determined from PN and particulate carbon (PC) concentrations), as well as the $\delta^{15}N$-PN, $\delta^{13}C$-PC and $\delta^{15}N\text{-}NO_3^-$ inside and outside Cyclone *Opal*. Using isotope inventories and a salt budget, we estimate the magnitude of nitrate injected during eddy formation, as well as the contribution of upwelled NO_3^- in supporting phytoplankton growth and export production. In addition, we compare NO_3^- assimilation and DON accumulation in order to elucidate the ultimate fate of the upwelled NO_3^- inside Cyclone *Opal*.

2. Methods

2.1. Field work and sample collection

Cyclone *Opal* appears to have formed between 2 and 18 February 2005 southwest of the Alenuihaha Channel (~20.3°N, 156.3°W) in the lee of the Hawaiian Islands. Spanning approximately 220 km in diameter (Dickey et al., 2008), Cyclone *Opal* was sampled repeatedly between 10 and 28 March 2005 (E-Flux III) onboard the R/V *Wecoma*. Data were collected from a subset of stations occupied during the field campaign and represent 12 stations at the center of Cyclone *Opal* (IN stations) and three control stations well outside the eddy path (OUT stations, Fig. 1 and Table 1). Not all properties were determined for each station (see Table 1). Hydrographic and bio-optical properties, as well as the history of formation and maturation of Cyclone *Opal*, are described in Dickey et al. (2008) and Nencioli et al. (2008). The center of Cyclone *Opal* was located using satellite imagery, sea-surface temperature (SST), density profiles, and an acoustic Doppler current profiler (ACDP) to map upper ocean currents. Measurements made at the IN stations represent a 9-day time series, providing valuable information on the physical and biogeochemical evolution of a mature eddy (Dickey et al., 2008; Rii et al., 2008; Brown et al., 2008). To be consistent with related work, mixed-layer depth (MLD, m) was defined as the depth at which seawater temperature was 1 °C less than the temperature at 10 m (Dickey et al., 2008; Nencioli et al., 2008).

Seawater from 0 to 1000 m was collected using a CTD/rosette package equipped with 12 10-l Niskin-like bottles (Dickey et al., 2008). Samples for NO_3^-, DON and $\delta^{15}N\text{-}NO_3^-$ were collected in acid-washed 125-mL HDPE screw top bottles, frozen upright immediately after collection and stored frozen at −20 °C until analysis. For PC and PN, 12 depths were sampled between 0 and 1000 m, and 2.2 L of seawater were filtered onto a combusted (450 °C for 4 h) 25-mm diameter Whatman GF/F filter. Filters were immediately wrapped in combusted foil and frozen at −20 °C until analysis.

2.2. Total and dissolved inorganic and organic nitrogen analysis

Concentrations of nitrate (NO_3^-, technically includes nitrite (NO_2^-), NO_2^- is generally found at nanomolar or sub-nanomolar concentrations and was not measured in this study) were determined using a Bran and Luebbe segmented flow auto-analyzer (Armstrong et al., 1967). The limit of detection for NO_3^- analysis by this procedure was 0.1 μM with a precision, based upon triplicate analysis of samples, of <1.5%. A five-point

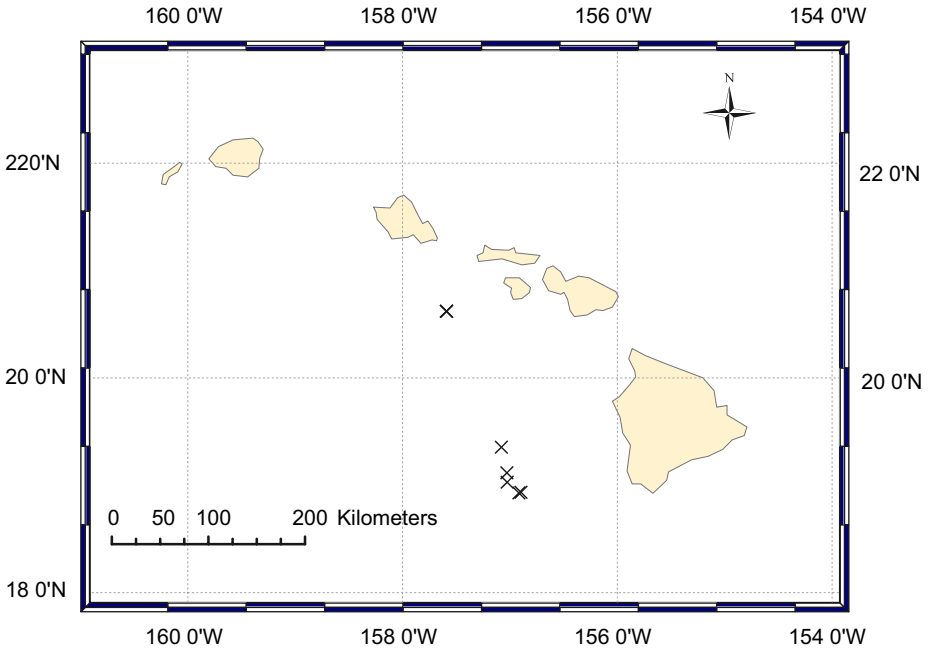

Fig. 1. Map of the Hawaiian archipelago and locations of stations inside Cyclone *Opal* (open circles) and outside Cyclone *Opal* (closed squares). Map prepared using Online Map Creation software at www.aquarius.geomar.de.

Table 1
Cast number, sample date, surface and integrated (0– 110 m) properties, ±standard error (S.E.) during E-Flux III for 12 stations inside and three stations outside Cyclone *Opal*

Cast	Date sampled	SST (°C)	MLD[a] (m)	DCML (m)	$\sigma_T = 24$ (m)	$Z_{nitrate}$[b] (m)	Nitrate (mmol m^{-2})	TDN (mmol m^{-2})	DON (mmol m^{-2})	PN (mmol m^{-2})	PC (mmol m^{-2})	δ^{15}N-PN (‰)	δ^{13}C-PC (‰)
IN_15	3/13/2005	24.80	97	120	61	35	n.d.	n.d.	n.d.	25.2±0.7	175.7±4.1	5.2±0.4	−21.2±0.2
IN_23	3/14/2005	24.67	90	95	42	n.d.	n.d.	n.d.	n.d.	27.7±1.0	175.4±6.1	6.8±0.6	−21.1±0.3
IN_49	3/16/2005	23.62	67	75, 94	55	32	96.4±6.4	n.d.	n.d.	42.7±3.1	306.9±18.0	2.5±0.3	−21.8±0.2
IN_63	3/17/2005	23.68	47	62	45	39	80.5±4.2	546.9±12.1	466.5±10.5	n.d.	n.d.	n.d.	n.d.
IN_67	3/18/2005	23.77	46	58	42	n.d.	n.d	498.3±14.6	406.8±8.5	n.d.	n.d.	n.d.	n.d.
IN_68	3/18/2005	23.87	45	71	49	45	71.6±6.5	n.d.	n.d.	30.1±1.7	228.2±9.2	5.0±0.8	−21.6±0.2
IN_73	3/19/2005	23.91	55	68	54	n.d	n.d	653.56±17.4	501.4±5.6	n.d.	n.d.	n.d.	n.d.
IN_74	3/19/2005	23.82	57	75	48	42	81.6±7.5	n.d.	n.d.	31.6±1.3	256.9±9.4	3.3±0.3	−22.1±0.5
IN_82	3/20/2005	23.91	55	73	52	n.d	n.d	517.5±9.9	424.5±7.2	n.d.	n.d.	n.d.	n.d.
IN_86	3/20/2005	23.90	50	70	49	43	112.3±10.1	n.d.	n.d.	n.d.	n.d.	n.d.	n.d.
IN_93	3/21/2005	24.01	48	75	48	48	72.5±8.1	n.d.	n.d.	n.d.	n.d.	n.d.	n.d.
IN_94	3/22/2005	24.01	55	78	53	n.d	n.d.	482.0±3.4	421.8±3.3	n.d.	n.d.	n.d.	n.d.
OUT_111	3/24/2005	25.18	94	102	128	121	8.5±0.2	467.9±12.3	440.6±11.9	30.4±0.9	234.2±6.9	2.4±0.4	−21.9±0.2
OUT_119	3/25/2005	25.10	90	111	123	119	11.6±0.3	433.6±9.9	415.4±9.3	28.2±1.4	165.4±5.2	5.8±0.3	−22.3±0.3
OUT_127	3/26/2005	24.80	103	123	127	118	33.5±1.0	444.3±9.2	421.4±9.2	n.d.	n.d.	n.d.	n.d.

Properties include sea-surface temperature (SST, °C), mixed layer depth (MLD, m), deep chlorophyll maximum layer (DCML, m), the depth of the $\sigma_T = 24.0$ m isopycnal, depth of the top of the nitricline ($Z_{nitrate}$, m), integrated concentration of nitrate (mmol m^{-2}), total dissolved nitrogen (TDN, mmol m^{-2}), dissolved organic nitrogen (DON, mmol m^{-2}), particulate nitrogen (PN, mmol m^{-2}) and carbon (PC, mmol m^{-2}). δ^{15}N-PN (‰) and δ^{13}C-PC (‰) are averaged after correction for N and C mass, respectively. Note that not all parameters were determined for each station (n.d.).

[a] Derived to be the depth at which seawater temperature was 1 °C less than the temperature at 10 m.

[b] The depth of the top of the nitricline ($Z_{NO_3^-}$, m) was determined by extrapolating the slope to zero NO_3^- between two depths (45 and 125 m inside and 125 and 250 m outside Cyclone *Opal* (Fig. 2).

calibration was performed using a sodium nitrate stock standard (10 mM) spiked into aged (>6 months) and filtered (0.2 μm) low-nutrient surface seawater. Accuracy was monitored by repeat analysis of a WACO CSK seawater standard (nitrate, 40-μM, #037-10241) and the coefficient of variation was typically less than 1.5%. The depth of the top of the nitricline ($Z_{NO_3^-}$, m, where NO_3^- concentrations approach undetectable levels μM) was determined by extrapolating the NO_3^- versus depth profile between 45 and 125 m inside Cyclone *Opal* and 125–250 m outside Cyclone *Opal* (Fig. 2A and B, respectively, Table 1). NO_3^- inventory was determined between 0 and 110 m, which approximately corresponds to the 1% light level at IN stations and matches the depth of integration used in related studies (Benitez-Nelson et al., 2007; Maiti et al., 2008).

Total dissolved nitrogen (TDN) concentrations were determined via high temperature combustion using a Shimadzu TOC-V with an attached Shimadzu TNM1 at the University of California, Santa Barbara (Carlson et al., 2004). Concentrations of DON were calculated as the difference between TDN and inorganic N (including NO_3^-, NO_2^- and NH_4^+, see Rii et al., 2008, for details).

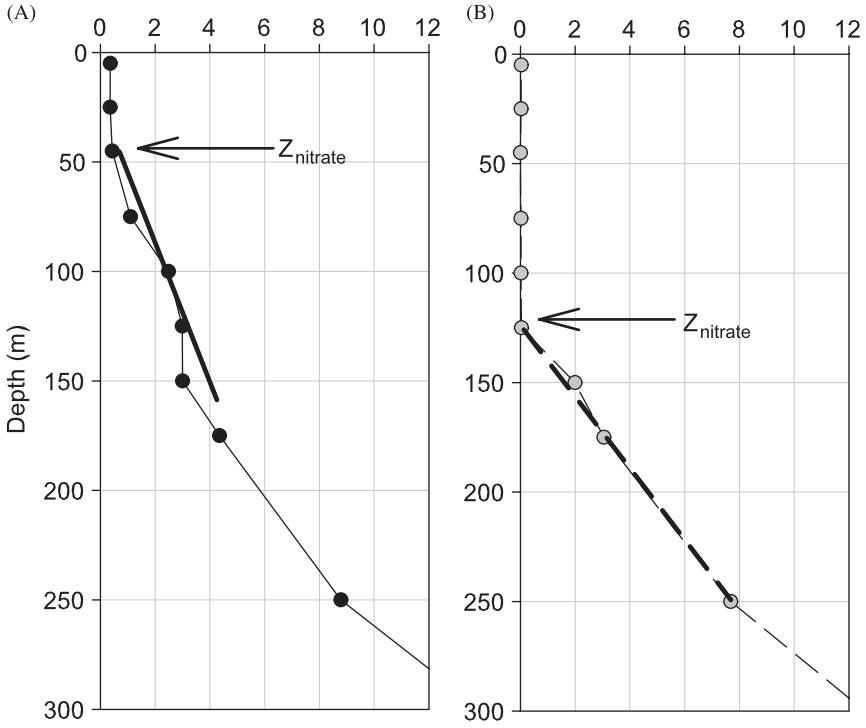

Fig. 2. Vertical distribution of nitrate concentrations (μM) for stations (A) inside and (B) outside Cyclone *Opal*. The solid line in (A) depicts a linear fit to the concentration of nitrate (NO_3^-) versus depth between 45 and 125 m inside Cyclone *Opal* used to derive the depth of the nitricline ($Z_{nitrate}$). The dashed line in (B) depicts a linear fit to the concentration of NO_3^- versus depth between 125 and 250 m in waters outside Cyclone *Opal* used to derive the depth of the nitricline ($Z_{nitrate}$).

All samples were systematically referenced against low-nitrogen, surface and deep (2600 m) Sargasso Seawater every 6–8 samples (Hansell and Carlson, 1998). Daily reference waters were calibrated with deep certified reference materials (CRM) provided by D. Hansell (University of Miami; Hansell, 2005).

2.3. Determination of the concentration and stable isotope composition of particulate nitrogen and carbon

Filters were removed from foil wraps, dried at 60 °C overnight and then pelletized in tin foil cups. Concentrations of PN, PC and stable N and C isotope ratios ($^{15}N/^{14}N$ and $^{13}C/^{12}C$, respectively) were determined using an elemental analyzer (Carlo Erba NC2500) coupled to an isotope ratio mass spectrometer (Thermo-Finnigan Delta S). The ratio of $^{15}N/^{14}N$ in a sample relative to the $^{15}N/^{14}N$ ratio in a standard (atmospheric N_2) is expressed as

$$\delta^{15}N = \left(\left(^{15}N/^{14}N\right)_{sample}\left(^{15}N/^{14}N\right)_{standard} - 1\right) \times 1000 \quad (1)$$

Commercially available standards (National Institute of Standards and Technology (NIST), IAEA-N1, IAEA-N2, USGS25 (ammonium sulfate) and N_3 (potassium nitrate)) were used to calibrate the N_2 standard and mass spectrometer. The ratio of $^{13}C/^{12}C$ relative to a standard (Vienna Peedee belemnite, VPDB) is expressed as $\delta^{13}C$, where

$$\delta^{13}C = \left(\frac{\left(^{13}C/^{12}C\right)_{sample}}{\left(^{13}C/^{12}C\right)_{standard}} - 1\right) \times 1000 \quad (2)$$

Throughout each analytical run, glycine was used as the elemental (C:N molar ratio = 2.0) and isotope standard ($\delta^{15}N = 11.25 \pm 0.15‰$, $\delta^{13}C = -35.81 \pm 0.2‰$). PN and PC concentrations were again integrated to 110 m at both IN and OUT stations. To determine the mean $\delta^{15}N$-PN and $\delta^{13}C$-PC in the top 110 m of the water column, the ^{15}N and ^{14}N, and ^{13}C and ^{12}C of a sample were corrected for its mass of N and C, respectively.

In order to estimate the magnitude of N and C downward particle flux, as well as the $\delta^{15}N$ of sinking PN, particle interceptor traps (PIT) were deployed at 150 m inside and outside Cyclone *Opal*. Details regarding PIT deployment, sample processing and analysis are outlined in Rii et al. (2008).

2.4. Determination of the stable N isotope composition of nitrate

The stable N isotope composition of nitrate ($\delta^{15}N$-NO_3^-) was determined using the "denitrifier" method originally developed by Christensen and Tiedje (1988) for freshwater and later adapted for seawater by Sigman et al. (2001) and Casciotti et al. (2002). This technique relies on the complete conversion of NO_3^- and NO_2^- to nitrous oxide (N_2O) by the denitrifying bacterium, *Pseudomonas chlororaphis*, that lacks N_2O reductase, the enzyme required for the final step in denitrification (reduction of N_2O to N_2). Cultures of *P. chlororaphis* were maintained at the University of Hawaii by M. Westley and N. Walsgrove following previously described guidelines (see Sigman et al., 2001, for details).

As recommended by Sigman et al. (2001), we used a 5-fold *P. chlororaphis* concentrate (cell counts not determined) to sample ratio of 4:1 for samples with sufficient NO_3^- to obtain a final N load of 10–20 nmol. In order to determine the $\delta^{15}N$ of samples in the upper water column where nitrate concentrations are less than 1 μM, the detection limit reported by Sigman et al. (2001), we adjusted the volume of concentrate and sample (but maintained a 4:1 ratio) to obtain sufficient nitrogen for $^{15}N_2O/^{14}N_2O$ determinations. In addition, the injection loop volume was adjusted (1–5 mL) to ensure sufficient loading of N for isotope analysis. With these refinements, we were able to achieve a detection limit of 0.4 μM. Sample N_2O gas was released from the sample vial by purging with helium for 8 min to fill the injection loop and 6 min to cryofocus the sample gas. The sample gas was injected into an in-house manufactured gas chromatograph through a Chrompak

PoroPLOT Q (25 m × 0.32 mm i.d.) coupled to a MAT252 mass spectrometer. The δ^{15}N-N_2O purged from the sample vial was standardized using a calibrated N_2O gas standard, NIST standards (IAEA-N3, potassium nitrate, δ^{15}N of 4.72‰) and a batch of seawater collected at 4000 m at station ALOHA (δ^{15}N of 5.6 ± 0.5‰). Based upon replicate analyses of NIST and deep seawater, the accuracy and precision of the δ^{15}N-NO_3^- method were ±0.3‰ and ±0.5‰, respectively.

3. Results

3.1. Hydrography, total and dissolved inorganic and organic nitrogen distributions

Cyclone *Opal* had distinct physical characteristics compared to surrounding waters (Table 1) (Nencioli et al., 2008). Mean sea-surface temperatures were significantly lower (by ~1 °C, $p<0.01$) at IN stations due to the uplift of cold and nutrient-rich deep waters, as evidenced by the average depth of the 24.5 kg m^{-3} density surface ($\sigma_T = 24.5$, 60 ± 7 m and 126 ± 2 m, respectively, Fig. 3A) and MLD (60 ± 5 m and 96 ± 4 m, respectively, Table 2). The mean deep chlorophyll maximum layer (DCML ± S.E.) was also uplifted by ~35 m at IN stations (77 ± 5 m, compared to 112 ± 6 m at OUT stations). Further details on the hydrography of Cyclone *Opal* are described by Dickey et al. (2008) and Nencioli et al. (2008).

During E-Flux III, NO_3^- concentrations did not exceed 0.36 μM above the depth of nitricline ($Z_{nitrate}$, see Table 1 for definition) at IN stations (41 ± 2 m), and was typically less than 0.1 μM (detection limit) above the $Z_{nitrate}$ at OUT stations (120 ± 1 m, Fig. 2 and Table 2). The integrated NO_3^- inventory in the upper 110 m was almost 5-fold higher at IN (85.8 ± 6.4 mmol m^{-2}) versus OUT stations (17.8 ± 7.8 mmol m^{-2}, $p<0.01$, Table 2), with the greatest increase in NO_3^- concentrations observed between 75 and 110 m. Comparison of NO_3^- concentration versus density (σ_T) demonstrates that the vertical distribution of NO_3^- was primarily controlled by the physical uplift of isopycnals associated with Cyclone *Opal* (Fig. 3C). NO_3^- concentration on the $\sigma_T = 24.4$ isopycnal is lower at IN stations ($\sigma_T = 24.4$ at 75 m) relative to OUT stations ($\sigma_T = 24.4$ at 150 m), reflecting biological uptake inside the eddy. Deeper in the water column ($\sigma_T = 25.0$–25.2), NO_3^- concentrations were lower at IN station relative to OUT stations, implying that either there were differences in the water properties along the isopycnals, reflecting translation of the eddy from its point of origin, or that the NO_3^-–density relationship was not resolved by the vertical spacing between the samples at OUT stations (Fig. 3C). In contrast, NO_3^- concentrations at $\sigma_T = 25.0$ were higher at IN stations relative to OUT stations. Implications of this observation are discussed further in Section 5.1.

Integrated (0–110 m) concentrations of TDN (±S.E.), (Fig. 4A, Table 2), were also significantly higher at IN stations (540 ± 30 mmol N m^{-2}) versus OUT stations (448 ± 10 mmol N m^{-2}, $p<0.01$), with most of this increase attributed primarily to NO_3^-. Indeed, integrated NO_3^- concentrations accounted for 35% and 9% of TDN at IN and OUT stations, respectively. There was no significant difference in the measured integrated DON concentrations (444 ± 18 mmol N m^{-2} at IN versus 425 ± 8 mmol N m^{-2} at OUT, Table 2, Fig. 4C).

3.2. Particulate carbon and nitrogen concentrations and δ^{13}C and δ^{15}N distributions

Concentrations of PN and PC were greatest in the upper portion of the water column and decreased rapidly below 100 m (Fig. 5A and B, respectively). No discernible difference in PN concentrations versus density surface was observed between IN and OUT stations (Fig. 5C). Depth integrated (0–110 m) concentrations (±S.E.) of PN and PC were similar at IN stations (31.5 ± 3.0 μM N and 228 ± 25.0 μM C, respectively) relative to OUT stations (29.3 ± 1.1 μM N and 199 ± 34.5 μM C, Table 2). Indeed, these inventories of particulate material are similar to those at the nearby time-series site, station ALOHA, where annual averaged

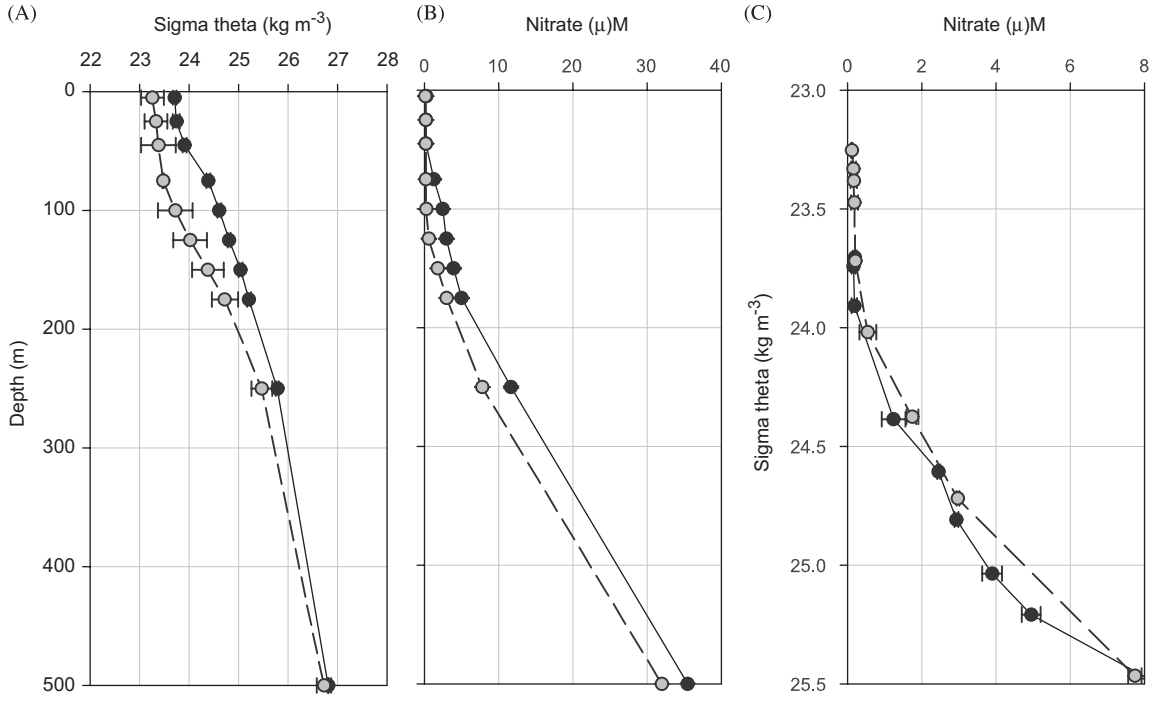

Fig. 3. Vertical distribution (0–500 m) of depth-averaged ± standard error of (A) sigma theta (σ_T, kg m^{-3}), (B) nitrate concentrations plotted against depth (μM) and (C) variation in nitrate concentrations with sigma theta (σ_T, sigma theta, kg m^{-3}) at stations sampled inside ($n = 6$, black circles) and outside ($n = 3$, gray circles) Cyclone *Opal*.

Table 2
Summary of the integrated properties (0–110 m) reported in Table 1, reported as mean ± standard error inside and outside Cyclone *Opal*

Parameter	Inside Cyclone *Opal*	Outside Cyclone *Opal*	Inside/Out	Significant difference (99%)
SST (°C)	24.0 ± 0.1	25.0 ± 0.1	0.96	Yes
MLD (m)	60 ± 5	96 ± 4	0.62	Yes
$\sigma_T = 24.0$ (m)	60 ± 7	126 ± 2	0.48	Yes
DCML (m)	77 ± 5	112 ± 6	0.69	Yes
$Z_{nitrate}$ (m)	41 ± 2	120 ± 1	0.34	Yes
1% light level (m)	110	150	0.73	n.d.
Nitrate (mmol m^{-2})	85.8 ± 6.4	17.8 ± 7.8	4.8	Yes
TDN (mmol m^{-2})	540 ± 30	448 ± 10	1.2	Yes
DON (mmol m^{-2})	444 ± 18	425 ± 8	1.04	No
PN (mmol m^{-2})	31.5 ± 3.0	29.3 ± 1.1	1.1	No
PC (mmol m^{-2})	228 ± 25	199 ± 34.5	1.1	No
δ^{15}N-PN (‰)	4.6 ± 0.8	4.1 ± 1.7	n.d.	No
δ^{13}C-PC (‰)	−21.6 ± 0.2	−22.1 ± 0.2	n.d.	No
PN export[a] (mmol N m^2 d^{-1})	0.15 ± 0.01	0.16 ± 0.02	0.94	No
δ^{15}N sinking PN[a] (‰)	4.5 ± 0.2	4.5 ± 0.4	n.d.	No
Nitrate assimilation rate[b] (mmol N m^{-2} d^{-1})	3.6 ± 1.7	n.d.	n.d.	n.d.
DON accumulation rate[c] (mmol N m^{-2} d^{-1})	0.83 ± 1.3	n.d.	n.d.	n.d.

The ratio of properties inside and outside the eddy is reported. Significance tests were conducted at the 99% confidence level.
[a] Rii et al. (2008), derived using sediment traps deployed at 150 m.
[b] Derived using the change in NO_3^- concentration estimated during eddy formation and that observed during E-Flux III (see Section 4.3).
[c] Derived using salinity mass balance of DON inside Cyclone *Opal* (see Section 4.3).

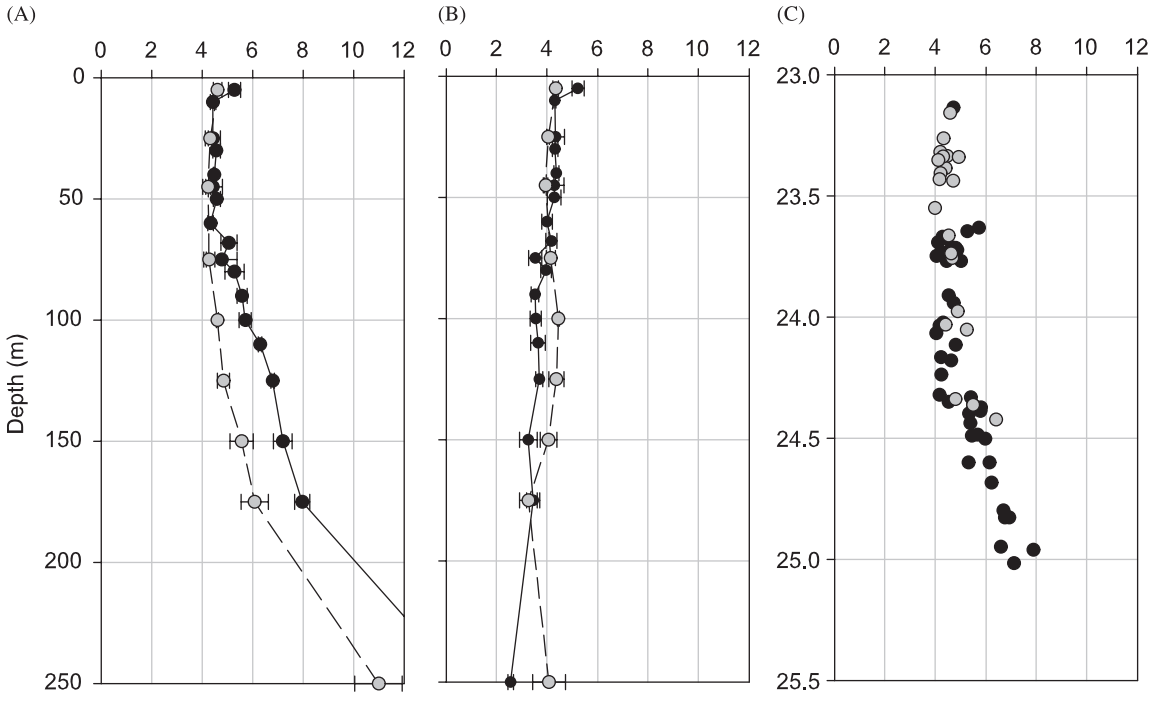

Fig. 4. Vertical distribution (0–250 m) of depth-averaged ± standard error of (A) concentrations of total dissolved nitrogen (TDN, μM) and (B) concentrations of dissolved organic nitrogen (DON, μM), and (C) variation in TDN concentrations with sigma theta (σ_T, kg m^{-3}) at stations sampled inside ($n = 5$, black circles) and outside ($n = 3$, gray circles) Cyclone *Opal*.

depth integrated PN and PC concentrations are 41.5 ± 2.0 mmol N m^{-2} and 264 ± 16 mmol C m^{-2} (http://hahana.soest.hawaii.edu/hot/hot-dogs/interface.html).

Mass-weighted mean distributions of δ^{15}N-PN and δ^{13}C-PC between 0 and 110 m were indistinguishable at IN (4.6 ± 0.8‰ and −21.6 ± 0.2‰, respectively) versus OUT stations (4.1 ± 1.7‰ and −22.1 ± 0.2‰, respectively, Table 2, Fig. 6). While there was a significant ($p < 0.01$) increase in the δ^{15}N-PN between 110 and 200 m at IN stations (5.4–9.5‰), PN became ^{15}N-deplete in this depth interval at OUT stations (down to 1.2‰, Fig. 6A). Below 200 m, δ^{15}N-PN reached similar values of 6–9‰ at both IN and OUT stations. Between the base of the mixed layer and 200 m, the δ^{13}C-PC of particles within Cyclone *Opal* remained relatively constant with depth, whereas particles sampled outside Cyclone *Opal* became relatively depleted in ^{13}C (< −23.0‰). Below 200 m, the δ^{13}C of particles were again similar at IN and OUT stations. There was no significant difference in the magnitude and δ^{15}N signature of sinking particulate matter captured by sediment traps deployed at 150 m at IN (0.15 ± 0.01 mmol N m^{-2} d^{-1} and 4.5 ± 0.2‰) and OUT stations (0.16 ± 0.02 mmol N m^{-2} d^{-1} and 4.5 ± 0.4‰) (Table 2, Rii et al., 2008).

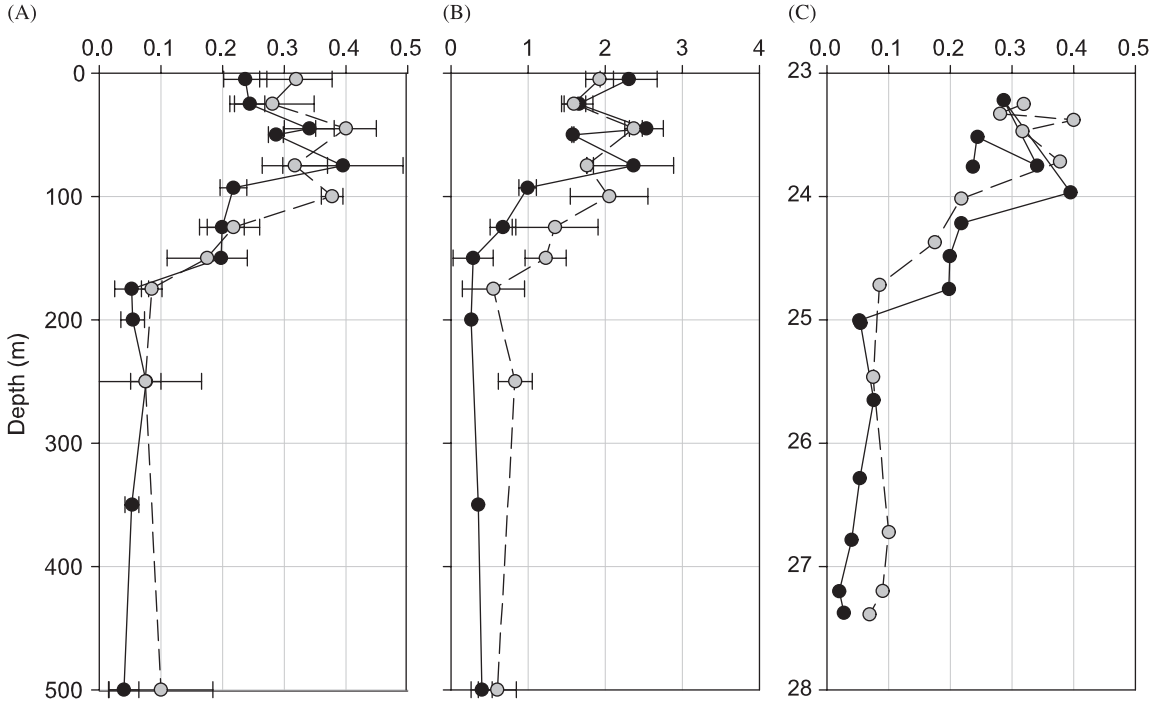

Fig. 5. Vertical distribution (0–500 m) of depth-averaged concentrations ± standard error of (A) particulate nitrogen (PN, μM), (B) particulate carbon (PC, μM) and (C) variation in PN concentrations with sigma theta (σ_T, kg m^{-3}) at stations sampled inside ($n = 5$, black circles) and outside ($n = 3$, gray circles) Cyclone *Opal*.

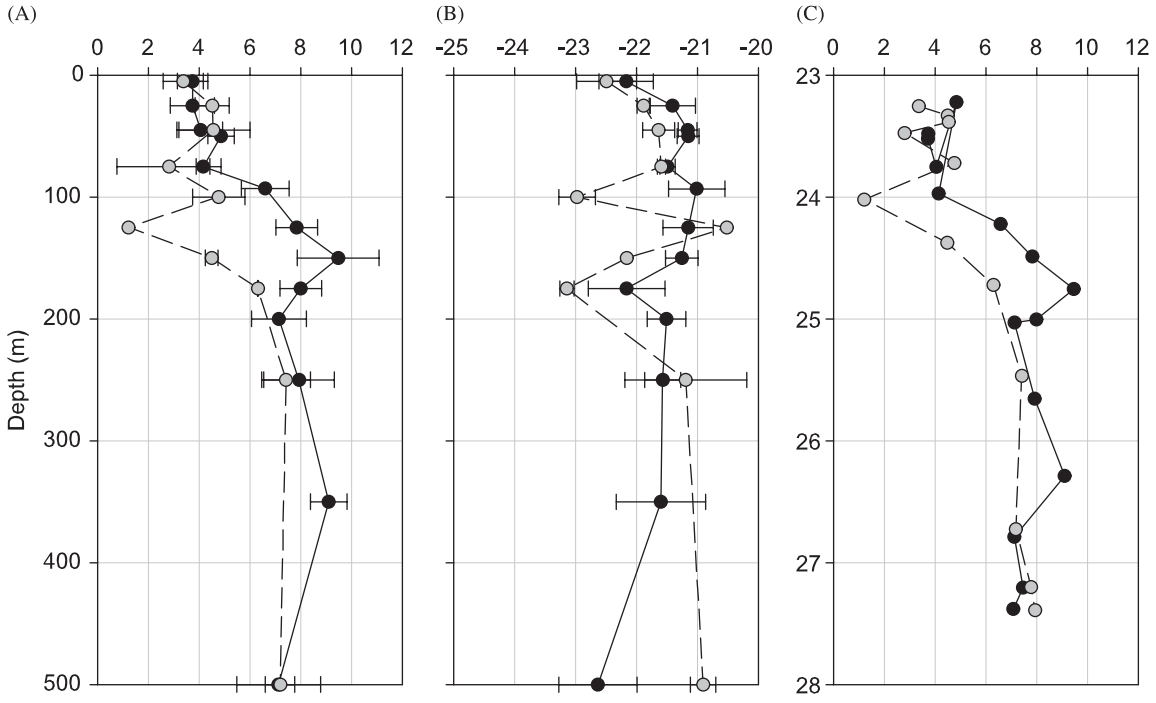

Fig. 6. Vertical distribution (0–500 m) of the stable isotope composition of (A) particulate nitrogen (δ^{15}N-PN, ‰) and (B) particulate carbon (δ^{13}C-PC, ‰) and (C) variation in the δ^{15}N-PN with sigma theta (σ_T, kg m^{-3}) at stations sampled inside ($n = 5$, black circles) and outside ($n = 3$, gray circles) Cyclone *Opal*.

3.3. $\delta^{15}N$–nitrate

Above the depth of the nitricline (41 ± 2 m at IN stations, 120 ± 1 m at OUT stations), concentrations of NO_3^- were generally too low to determine the δ^{15}N-NO_3^- (limit of detection, 0.4 μM). The δ^{15}N-NO_3^- was most variable in the upper 200 m of the water column (Fig. 7A and B), and diverged significantly above the $\sigma_T = 24.5$ isopycnal at IN and OUT stations (Fig. 7C). Above the MLD (60 m) at IN stations, δ^{15}N-NO_3^- ranged from 11.1‰ to 15.5‰, with a mean of 12.4 ± 1.6‰. Just below MLD, the δ^{15}N-NO_3^- decreased to a minimum of 4.4‰ (at 75 m). At OUT stations, a minimum in δ^{15}N-NO_3^- of 1.69‰ was observed at the depth of the MLD (96 m), with a gradual increase in δ^{15}N-NO_3^- to >6‰ at 175 m. This sub-euphotic minimum in δ^{15}N-NO_3^- has been

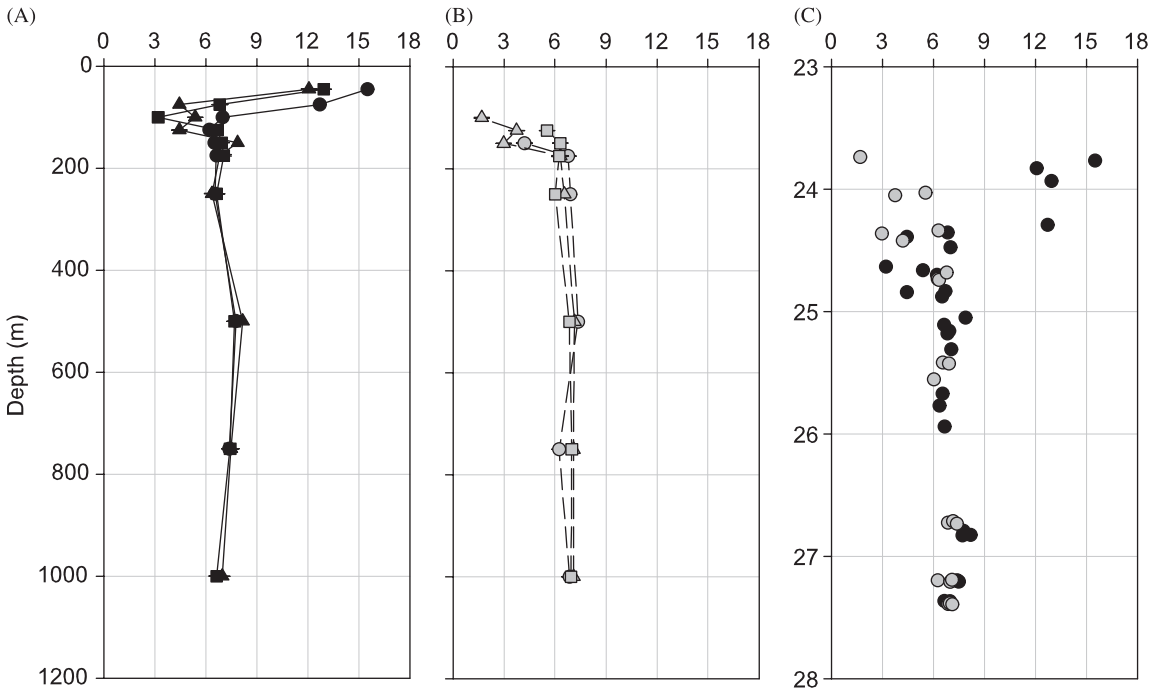

Fig. 7. Vertical distribution (0–1000 m) of the stable nitrogen isotope composition of nitrate (δ^{15}N-NO_3^-, ‰) (A) inside Cyclone *Opal* (black symbols), (B) outside Cyclone *Opal* (gray symbols) and (C) variation of δ^{15}N-NO_3^- with sigma theta (σ_T, kg m^{-3}).

observed in other studies (Liu et al., 1996; Sutka et al., 2004; Knapp et al., 2005). Below the MLD, δ^{15}N-NO_3^- was relatively uniform at IN (7.19 ± 0.59‰) and OUT (6.84 ± 0.39‰) stations and similar to previous δ^{15}N-NO_3^- measurements in the upper thermocline of the Pacific Ocean (6–7‰, Cline and Kaplan, 1975; Altabet, 2001; Sutka et al., 2004; Sigman et al., 2005).

3.4. Time-series observations within Cyclone Opal

Stations within Cyclone *Opal* were sampled from 13 to 22 March 2005, providing a 9-day time series. From day 1 to day 4, we observed a decrease in SST (from 24.80 °C to a minimum of 23.62 °C, note that Cyclone *Opal* was not detected from satellite derived sea surface imagery), shallowing of the MLD (from 97 m to a minimum of 45 m) and a small change in $Z_{NO_3^-}$ (from 35 to 45 m) (Fig. 8A, Table 1). This change in the physical structure of the water column was accompanied by a significant ($p < 0.01$) increase in the 110 m integrated concentrations of PN (25.0 ± 0.7 to 42.7 ± 3.1 mmol N m^{-2}) and PC (175.7 ± 4.1 to 306.9 ± 18.0 mmol C m^{-2}) (Fig. 8B), and a significant decrease in the δ^{15}N-PN (from 5.2 ± 0.4‰ to 2.5 ± 0.3‰) (Fig. 8C). From day 4 to day 7, there was a significant ($p < 0.01$) decrease in PN and PC, and an increase in the δ^{15}N-PN. The implications of these observations are discussed below (Section 5.3).

4. New, export and net community production

Eddies can enhance the NO_3^- inventory in the euphotic zone by upwelling nutrient-rich deep waters from below, thereby enhancing growth and promoting a shift in community structure from small to large photoautotrophs (Sweeney et al., 2003; McGillicuddy et al., 2007). Assuming steady state, the input of new NO_3^- into the euphotic zone should be approximately equal to the downward PN flux plus the accumulation of DON and suspended particles (Eppley and Peterson, 1979; Laws, 1991). In this section, we will attempt to (1) estimate the magnitude of the NO_3^- pool injected during eddy formation, (2) estimate the contribution of injected NO_3^- that supports Cyclone *Opal* plankton growth and particle export, and (3) estimate the rate of NO_3^- assimilation versus DON accumulation.

4.1. Nitrate inventory inside Cyclone Opal

During E-Flux III, the NO_3^- inventory above 110 m was 4.8 times greater at IN stations (85.8 ± 6.4 mmol N m^{-2}) relative to OUT stations (17.8 ± 7.8 mmol N m^{-2}) (Table 2), implying that there is 68 ± 10 mmol N m^{-2} of excess NO_3^- inside Cyclone *Opal* when sampled in March 2005. If we assume that Cyclone *Opal* consisted of one injection of nutrient-rich deep water rather than a continuous supply (Nencioli et al., 2008), then this residual NO_3^- pool represents the fraction of the initially injected NO_3^- that remained unassimilated. Here, we attempt to calculate the magnitude of NO_3^- injected during the spin-up of Cyclone *Opal*.

At IN stations, we observed an ^{15}N-enrichment (mean δ^{15}N-NO_3^- of 12.4 ± 1.6‰) of the upper water-column NO_3^- pool that is characteristic of isotope discrimination during NO_3^- drawdown (Fig. 7, Altabet, 2001). We therefore used this information to estimate *f*, the fraction of unassimilated NO_3^-, according to Rayleigh fractionation kinetics:

$$\delta^{15}N_{NO_3^-\ euphotic} = \delta^{15}N_{NO_3^-\ initial} - \varepsilon(\ln f), \quad (3)$$

where $\delta^{15}N_{NO_3^-\ euphotic}$ is the δ^{15}N of the NO_3^- pool in the surface, $\delta^{15}N_{NO_3^-\ initial}$ is the δ^{15}N of the NO_3^- supplied to the surface ocean (6.8‰, the δ^{15}N-NO_3^- at 1000 m, see Section 5), ε is the kinetic isotope effect (5‰ for NO_3^-, Waser et al., 1998; Altabet, 2001) and *f* is the fraction of the initial NO_3^- pool remaining in the surface ocean. Using Eq. (3), we calculate *f* to be 0.32 ± 0.06, implying that 68 ± 12% of the supplied NO_3^- had been assimilated. In other words, the excess NO_3^- inventory inside the eddy reflects 32% of the initial NO_3^- injection. We thus estimate that the total NO_3^- injected by Cyclone *Opal* by scaling the net difference between IN

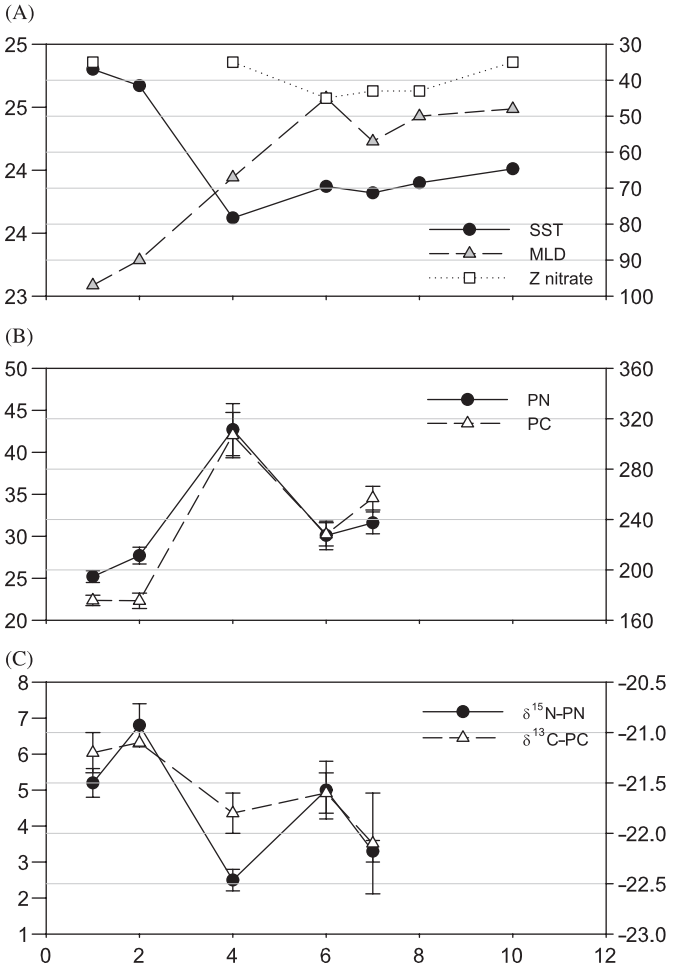

Fig. 8. Temporal variation in (A) mixed-layer depth (MLD, m), sea-surface temperature (SST, °C) and depth of the nitricline ($Z_{nitrate}$, m), (B) particulate nitrogen (PN, mmol N m^{-2}) and particulate carbon (PC, mmol C m^{-2}) concentrations integrated above 110 m (see Table 1), and (C) the stable isotopic composition of PN (δ^{15}N-PN, ‰) and PC (δ^{13}C-PC, ‰) inside Cyclone *Opal* between 13 and 22 March 2005.

and OUT inventories (68 ± 10 mmol N m^{-2}) accordingly, which results in 213 ± 59 mmol N m^{-2}. This is 1.4 times greater than that determined from Benitez-Nelson et al. (2007) who used a salinity mass balance approach to suggest that 147 ± 32 mmol m^{-2} of NO_3^- was initially injected above 110 m during the spin-up of Cyclone *Opal*.

4.2. Contribution of upwelled nitrate to nitrogen demand and export production

Using a two end-member-mixing model, one can estimate the relative importance of new N in fueling phytoplankton growth and export production by balancing the relative contribution of the N source and its δ^{15}N signature with the δ^{15}N of the suspended or sinking particles. For example, if 100% of new and export production is supported by NO_3^- and there is no isotopic fractionation associated with NO_3^- assimilation, the δ^{15}N of suspended and sinking particles will be equal to the δ^{15}N-NO_3^- supplied. Assuming that N_2 fixation (0 ± 0.2‰) and NO_3^- from the deep ocean (6.8 ± 0.5‰, Section 3.3) represent the two new N-source end members in this oligotrophic region, and the error in the analysis of δ^{15}N-PN is ± 0.2‰, then we can estimate that the upwelled NO_3^- inside Cyclone *Opal* supplies 68 ± 19% of the surface N-demand (suspended particles, 4.6 ± 0.8‰, Table 2) and 66 ± 9% of the N exported from the surface ocean (sinking particles, 4.5 ± 0.2‰, Table 2). Errors bars reported represent analytical errors associated analysis of δ^{15}N-PN and δ^{15}N-NO_3^-. However, variations in the δ^{15}N-NO_3^- will alter the contribution of NO_3^- in fuelling phytoplankton growth and export (see Section 5.2).

4.3. Nitrate consumption and DON accumulation inside Cyclone *Opal*

Cyclone *Opal* was estimated to be 4–6 weeks old when sampled in March 2005. In Section 4.1, we determined the initial NO_3^- inventory inside Cyclone *Opal* to be 213 ± 59 mmol N m^{-2}, implying that 127 ± 59 mmol N m^{-2} of NO_3^- were assimilated during the 4–6 weeks lifetime of the eddy (initial estimated versus actual measured: 213–86 mmol N m^{-2}). Assuming that the injection of nutrient-rich deep water into the upper 110 m occurred only during the spin-up of Cyclone *Opal*, and assimilation of NO_3^- by phytoplankton is constant, we estimate that NO_3^- was consumed at a rate of 3.6 ± 1.7 mmol N m^{-2} d^{-1}. In essence, this is equivalent to nitrate-derived new production. This is double the average net community production estimated for Cyclone *Opal* using a salinity mass approach to derive a net community production of 1.8 ± 0.7 mmol N m^{-2} d^{-1} (assuming a C:N ratio of 6.6, Chen et al., 2008), but they are statistically indistinguishable.

In order to determine the change in the DON inventory from the spin-up of Cyclone *Opal* to the time of sampling in March 2005, we need to estimate the initial DON concentration during eddy formation. Briefly, we employed a salt budget to derive the initial composition of the seawater within the photic zone of the eddy core (see Benitez-Nelson et al., 2007; Chen et al., 2008). This calculation takes into account the dilution effect created by the upward injection of lower salinity, high-NO_3^-, lower DON waters from below. In the upper 110 m of the water column, the initial weighted average DON concentration (integrated DON concentration divided by 110 m) at IN stations was 3.78 ± 0.40 mmol m^{-3}. The observed weighted average DON concentration over the upper 110 m was 4.04 ± 0.09 mmol m^{-3} (Table 2), implying that 0.26 ± 0.4 mmol m^{-3} or 29 ± 44 mmol m^{-2} of DON accumulated over the top 110 m over 4–6 weeks inside the eddy. Thus, we estimate that DON was produced at a rate of 0.83 ± 1.3 mmol N m^{-2} d^{-1} (29 mmol m^{-2} divided by 28–42 days), which is not significantly different from zero when errors are considered.

5. Discussion

5.1. Distribution of nitrogen inside Cyclone Opal

Significant increases in autotrophic biomass (chlorophyll *a*) and a dominance of large siliceous diatoms were observed within Cyclone *Opal* (Benitez-Nelson et al., 2007; Brown et al., 2008; Rii et al., 2008) in response to the upwelling of nutrient-rich deep waters into the euphotic zone. Inside Cyclone *Opal*, there was a 4.8-fold increase in integrated NO_3^- concentrations (85.8 ± 6.4 mmol N m^{-2}) in the upper 110 m relative to the surrounding water column when sampled in March 2005. We infer that during eddy formation, integrated NO_3^- concentrations were almost 12-fold higher (213 ± 59 mmol NO_3^- m^{-2}) than typically found in this region of the Pacific Ocean. This is similar to previous observations in Hawaii Cyclones *Mikalele* and *Loretta,* which exhibited a 3- and 15-fold increase in NO_3^- concentrations (Seki et al., 2001). Surprisingly, however, there were no significant

differences in the integrated suspended PN and PC concentrations at IN versus OUT stations during E-Flux III. In addition, three independent techniques used to determine Cyclone *Opal* export production revealed no significant increase in the sinking particle flux of PN or PC (see Table 2, Rii et al., 2008; Maiti et al., 2008; Benitez-Nelson et al., 2007). Rather, Cyclone *Opal* acted as a selective silica pump, exporting empty diatom frustules (Benitez-Nelson et al., 2007). In fact, there was no significant difference in export production found inside Cyclone *Opal* relative to station ALOHA, the nearby time-series station (Benitez-Nelson et al., 2001). Therefore, we must consider the fate of NO_3^- injected into Cyclone *Opal*.

From Section 4.1, we estimate that 213 ± 59 mmol m^{-2} of NO_3^- was injected into Cyclone *Opal* during its formation and was assimilated at a rate of 3.6 ± 1.7 mmol N m^{-2} d^{-1}. However, 4–6 weeks after formation, 32 ± 6% of the initial NO_3^- injected remained unassimilated. The lack of significant suspended particle accumulation (this study) or significant sinking particle flux (Benitez-Nelson et al., 2007; Rii et al., 2008; Maiti et al., 2008), implies that the NO_3^- injected into Cyclone *Opal* potentially accumulated as some other N species. In Section 4.3, we estimated that DON was produced at a rate of 0.83 ± 1.3 mmol N m^2 d^{-1}, with total DON accumulation of 0.26 ± 0.4 mmol N m^{-3}. If we compare the accumulation of DON to the pool of assimilated NO_3^- (127 ± 59 mmol N m^{-2} divided by 110 m $= 1.2 \pm 0.5$ mmol N m^{-3}), we find that DON accounts for 22 ± 15% of the injected NO_3^- pool within Cyclone *Opal*. Thus, N mass balance reveals that, after accounting for the percentage of NO_3^- remaining (32 ± 6%), and that percentage of NO_3^- that was shunted into the DON pool (22 ± 15%), 46 ± 16% (or 98 ± 34 mmol N m^{-2}) of the injected NO_3^- is unaccounted for. Considering that no significant particle accumulation or export was observed within Cyclone *Opal*, alternative sinks and loss processes must be considered.

Within Cyclone *Opal*, an increase in the abundance of diatoms is reported to have enhanced grazer biomass by up to 6 times compared to surrounding waters (Brown et al., 2008), reflecting a predator–prey response within the eddy. Indeed, grazing by microzooplankton was found to consume 55% of the total phytoplankton community production within Cyclone *Opal* (Landry et al., 2008). Considering the lack of substantial zooplankton-derived particle export at 150 m (i.e. fecal pellets), PN consumed by zooplankton may have been exported below the 150 m depth of the sediment traps by active migration. There is no evidence for accumulation of NH_4^+ inside Cyclone *Opal*. Another possibility is advection or mixing. Nencioli et al. (2008) report that within Cyclone *Opal*, there was radial exchange between the center of the eddy and the surrounding water column along the $\sigma_T = 23.6$ and 24.4 density surfaces (corresponding to 70–90 m at the eddy center). Exchange between the eddy center and surrounding and underlying waters may have potentially facilitated lateral net loss of NO_3^- from within Cyclone *Opal* (see Section 5.3).

It is interesting to note that despite Cyclone *Opal* being 4–6 weeks old, not all the NO_3^- injected had been consumed. There are a number of possible explanations. In the deeper region of the euphotic zone, significant light limitation may inhibit autotrophic NO_3^- uptake due to accumulation of phytoplankton biomass in the upper euphotic zone (i.e. self-shading), as observed during E-Flux III (Brown et al., 2008). However, it is known that some diatoms are capable of growing at near their maximal rates at irradiances characteristic of the lower euphotic zone (Goldman and McGillicuddy, 2003). Also, both indirect (physical model, Martin and Pondaven, 2003) and direct (^{15}N incorporation, Allen et al., 1996) studies have concluded the efficiency in transferring N from NO_3^- to particulate export within cyclonic eddies is highly variable (10–77%). Depletion of a specific nutrient other than N inside Cyclone *Opal* also may have led to a lack of complete N assimilation (see Section 5.3).

As noted in Section 3.1, NO_3^- concentrations at $\sigma_T = 26.8$ (~500 m) are significantly higher at IN stations relative to OUT stations. This potentially reflects remineralization at depth. For example, excess NO_3^- at 500 m is approximately 3 mmol m^{-3}. Therefore, only a 32-m thick layer of water could account for the entire 98 ± 34 mmol m^{-2} of missing N. Unfortunately, the vertical resolution of NO_3^- sampling was insufficient to characterize this feature in detail and there is no clear supporting evidence that remineralization occurred. Oxygen profiles over the same depth range show no significant differences in concentration between IN and OUT stations (<5 μM O_2, Nencioli et al., 2008). Excess dissolved inorganic carbon (DIC) concentrations are too noisy to resolve a ~20 μM DIC signal (Chen et al., 2007) and ^{234}Th measurements, although coarse, give no clear indication of excess ^{234}Th at that depth (Maiti et al., 2008).

5.2. Distribution of ^{15}N and ^{13}C inside Cyclone Opal

Suspended particles inside Cyclone *Opal* were ^{15}N-enriched compared to typical oligotrophic waters (<2‰, Checkley and Miller, 1989), reflecting assimilation of ^{15}N-enriched NO_3^- within a closed system. These observations are in concordance with studies by Waser et al. (2000) and Mahaffey et al. (2004), who hypothesized that ^{15}N-enriched phytoplankton (>3‰) in the North Atlantic were due to assimilation of NO_3^- from the deep ocean that had been injected into the surface by some physical process, such as eddies or Rossby waves. According to Waser et al. (2000), changes in the rate of NO_3^- supply and its δ^{15}N-NO_3^- are the principle factors controlling variations in δ^{15}N of suspended PN in the surface ocean. In addition, they concluded that seasonal variability in the δ^{15}N-NO_3^- supplied to the surface ocean was primarily responsible for the basin scale change in δ^{15}N-PN between spring and fall in the North Atlantic. A time-series study of δ^{15}N-NO_3^- showed significant seasonal variation in sub-euphotic (250 m) δ^{15}N-NO_3^- at the Bermuda Atlantic Time-series Study site (BATS) in the subtropical North Atlantic (Knapp et al., 2005), with δ^{15}N-NO_3^- being <2.5‰ during the summer months, and >2.5‰ during the winter months. Unfortunately, there are no supporting or published δ^{15}N-PN data (suspended or sinking) to examine the effect of variations in δ^{15}N-NO_3^- on the δ^{15}N of suspended or sinking material at BATS.

Between 75 and 200 m, the δ^{15}N-NO_3^- differs between IN and OUT stations. Outside the eddy, NO_3^- was ^{15}N-depleted (to ~1‰) relative to the δ^{15}N-NO_3^- of deep water (~6.8‰). This appears to be a common feature at the base of the euphotic zone and may be due to remineralization of ^{15}N-depleted sinking PN from N_2 fixation (Liu et al., 1996), oxidation of semi-labile total organic nitrogen (TON) (Knapp et al., 2005) or nitrification. In fact, nitrification, the microbial-mediated conversion of NH_4^+ to NO_3^-, is a highly fractionating process (35‰, Casciotti et al., 2003; Sutka et al., 2004) that has the potential to deplete the ^{15}N of the NO_3^- produced (although this pool is likely small and short lived). In addition, nitrification also complicates our understanding of new versus regenerated nitrogen as NO_3^- produced through this process is essentially regenerated and may represent up to 80% of NO_3^- in the euphotic zone (Lipschultz et al., 2002; Martin and Pondaven, 2003, 2006). Thus, outside the path of Cyclone *Opal*, any of these processes may have contributed to the observed trends in δ^{15}N-NO_3^-. In contrast, at IN stations, δ^{15}N-NO_3^- at the base of the euphotic zone was always greater than 4.4‰. This implies that the rate of NO_3^- supply at the base of the euphotic zone was sufficient to mask the isotope effects associated with processes that act to deplete NO_3^- in ^{15}N, or dilute the pool

of ^{15}N-depleted NO_3^-. In this study, we assumed an initial and constant $\delta^{15}N_{initial}$ of NO_3^- (6.8‰, $\delta^{15}N$-NO_3^- at 1000 m) at both IN and OUT stations. However, if the $\delta^{15}N$-NO_3^- is <6.8‰, the contribution of deep NO_3^- to supporting new and export productivity (as estimated in Section 4.1), e.g., the *f*-value or the fraction of unassimilated NO_3^-, would decrease.

In this same region of the water column (100–200 m), there was also a significant ^{15}N-enrichment in suspended PN observed inside Cyclone *Opal*. This ^{15}N-enrichment of particles in the sub-euphotic region (150–200 m) and indeed in the "twilight" zone (~200–1000 m) inside Cyclone *Opal* probably reflects the loss of ^{15}N-depleted proteins and nucleic acids during remineralization and ammonification of particulate matter during sinking (Altabet et al., 1986; Macko et al., 1987; Altabet, 1988). This is further supported by ^{234}Th flux data of Maiti et al. (2008) who concluded that there was intense remineralization between 100 and 150 m.

During E-Flux III, the $\delta^{15}N$-PN of sinking PN also was determined using material captured in sediment traps deployed at 150 m. There appears to be little difference in $\delta^{15}N$ of sinking PN captured inside (4.5 ± 0.2‰) and outside (4.5 ± 0.4‰) Cyclone *Opal* (Table 2). Interestingly, the $\delta^{15}N$ of sinking PN is similar to the $\delta^{15}N$ of suspended PN at IN (4.6 ± 0.8‰) and OUT (4.1 ± 1.7‰) stations as well. Altabet (2001) found a similar relationship between $\delta^{15}N$ of sinking PN and $\delta^{15}N$ of suspended PN in the NO_3^--dominated equatorial upwelling region of the tropical Pacific Ocean and interpreted this similarity as demonstrating a tight coupling between euphotic zone processes and particles at depth when NO_3^- is the dominant nutrient. In addition, recent evidence suggests that remineralization of diatom bound organic matter, specifically amino acids, occurs as a result of mineral rather than organic matter remineralization, implying that organic matter associated with rapidly sinking diatom frustules is preserved (Ingalls et al., 2006).

It is important to note that ^{15}N-enriched suspended PN also can be generated by inclusion of higher trophic levels during sampling, which tend to be enriched by 2–3.5‰ relative to their food source (Checkley and Miller, 1989). Enhanced microzooplankton biomass was observed inside Cyclone *Opal* (Landry et al., 2008) and in cyclonic and mode water eddies sampled in the Sargasso Sea (Goldthwait and Steinberg, 2008). Therefore, inclusion of zooplankton cannot be disregarded as a factor responsible for the ^{15}N-enriched suspended PN observed within Cyclone *Opal*.

Considering the spectrum of processes that can potentially alter the $\delta^{13}C$ of phytoplankton (see Section 1), the general consistency of $\delta^{13}C$-PC both inside and outside Cyclone *Opal* suggests that any change in growth rates or productivity induced by Cyclone *Opal* was insufficient to alter the carbon chemistry. In fact, Chen et al. (2007) suggest that Cyclone *Opal* is 17% less of a CO_2 sink than surrounding waters due to upwelling of DIC-rich deep waters.

5.3. Temporal dynamics and nutrient limitation inside Cyclone Opal

During E-Flux III, Cyclone *Opal* was sampled over a 9-day period, thus providing rare insight into temporal changes in water-column properties, particulate inventories and stable isotopic signatures inside a mature cyclonic eddy. From Fig. 8A, it appears that an increase in water-column stability, probably signaling the relaxation of isopyncals inside Cyclone *Opal*, coincided with a significant increase in particulate nitrogen in the upper ocean from day 1 to day 4. Enhanced phytoplankton growth may be responsible for this increase in PN although patchiness in sampling cannot be ruled out. Depletion in ^{15}N-signatures during this period implies that there was an apparent change in the nutrient source or dynamics. There are a number of possible explanations for this observation. Increased ^{15}N discrimination (i.e. an increase in the ε) associated with the uptake and assimilation of a single nutrient source (e.g. NO_3^-) may be responsible for the ^{15}N-depletion of phytoplankton. Alternatively, there may have been a change in the N source to phytoplankton within Cyclone *Opal*, from a ^{15}N-enriched source, NO_3^-, to a ^{15}N-depleted source. An increase in zooplankton biomass and grazing may lead to an increase the availability of ^{15}N-depleted NH_4^+, which could be readily assimilated by phytoplankton. The rapid shift in Cyclone *Opal* community structure during the time-series observation supports an increase in the abundance of diazotrophs and thus assimilation of N_2 gas, resulting in exudation of ^{15}N-deplete dissolved N (Brown et al., 2008). Rates of N_2 fixation were not determined during E-Flux III and our observations represent one data point on one day, with $\delta^{15}N$-PN returning to more enriched values after day 4. Therefore, these observations should be treated with caution as spatial heterogeneity cannot be dismissed.

It is interesting to note that despite an increase in particulate biomass over 4 days, sediment traps and ^{234}Th-derived particle export increased only minimally, if at all (Rii et al., 2008; Maiti et al., 2008). Laws et al. (2000) suggest that above 25 °C, the export ratio, defined as the ratio of new or export production to total production, is relatively insensitive to changes in total production. Experimental manipulations of the plankton community inside Cyclone *Opal* resulted in a simultaneous decrease in gross primary production and community respiration 72 h after nutrient additions, implying that the system rapidly adjusts its metabolic balance to maintain steady state (McAndrew et al., 2008).

High-resolution mooring-based observations in both the Atlantic (Bermuda test-bed mooring; McNeil et al., 1999) and Pacific Oceans (HALE ALOHA; Sakamoto et al., 2004; Letelier et al., 2000) have demonstrated that there are complex temporal dynamics between the delivery of NO_3^- and the biological response generated by a passing cyclonic eddy. At the HALE ALOHA mooring, a 3-fold increase in NO_3^- concentrations (1.96 ± 1.09 to $5.48\pm0.54\,\mu mol\,kg^{-1}$) was observed in response to a change in sea surface height, followed rapidly (~72 h) by an increase in chlorophyll *a*, which was sustained for up to 1 month following the increase in NO_3^-. At the Bermuda test-bed mooring in the subtropical North Atlantic, McNeil et al. (1999) observed a rapid increase in chlorophyll *a* (maximum of $1.4\,mg\,m^{-3}$) 2 days after an initial NO_3^- injection, with enhanced biological activity maintained for the following 8 days. It is possible that prior to sampling Cyclone *Opal* in March 2005, the maximum NO_3^- loading, as well as biological response and biomass accumulation, may have already occurred, hence the relatively low suspended particulate biomass relative to surrounding waters. However, if this were correct, we may expect to see remnants in the downward particulate flux and there is no evidence of a substantial downward particle flux prior to sampling from ^{234}Th–^{238}U and ^{210}Po–^{210}Pb disequilibrium measurements (Benitez-Nelson et al., 2007; Maiti et al., 2008; Verdeny et al., 2008).

Nutrient limitation or a shift in nutrient stoichiometry may also help to explain the lack of significant PN accumulation and the contrast in $\delta^{15}N$ signatures inside Cyclone *Opal*. Altabet (2001) observed no change in ^{15}N distribution in the equatorial Pacific region, despite a doubling of NO_3^- supply and concluded that iron was limiting NO_3^- uptake. In this study, it has been proposed that silicic acid may have been limiting inside Cyclone *Opal* during the time period of observation and may have driven the community transition from diatoms to other plankton assemblages, such as *Prochlorococcus* spp. (Benitez-Nelson et al., 2007; Brown et al., 2008). In addition, the N:P ratio of the underlying nutrient pool is <12 in the upper 200 m, and ~14 at 1000 m (Rii et al., 2008), suggesting that if plankton were assimilating phosphate and NO_3^-

at Redfield proportions (16:1; Redfield, 1958), NO_3^- would be depleted before phosphate, leaving an excess phosphate pool. This scenario is thought to promote N_2 fixation at station ALOHA (Karl et al., 2008) and across much of the eastern Pacific (Deutsch et al., 2007).

Although we attempt to classify Cyclone *Opal* as a closed system with respect to N isotope discrimination, it is likely that eddies are open systems during formation but possibly vertically segregated throughout their lifetime (Chen et al., 2008; Nencioli et al., 2008). An early study on Hawaiian lee eddies by Patzert (1969) concluded that within a cyclonic eddy, upwelling occurs during the formation stage only and despite a significant upward vertical velocity (10^{-2} cm s^{-1}), nutrient enrichment is confined to deeper layers of the water column (unless there is outcropping at the surface). Nencioli et al. (2008) described Cyclone *Opal* as a shallow, open-bottom and horizontally leaky eddy, with only a small (50 km in diameter) and relatively shallow (to a depth of 70 m) isolated region. Such exchange or connectivity of Cyclone *Opal* with the surrounding and underlying water column may potentially facilitate lateral net losses of NO_3^- and DON, thus serving to close the N budget within Cyclone *Opal*. However, such connectivity may also potentially drive additional inputs of NO_3^- after the formation of the eddy, which would affect not only the biogeochemistry within Cyclone *Opal* (e.g. by enhancing or suppressing a phytoplankton bloom), but also N isotope distribution. If the upper 70 m of the eddy received multiple sporadic injections of NO_3^- from the deep ocean during its lifetime, and the rate of supply was significantly greater than the rate of autotrophic assimilation, we would expect the observed δ^{15}N-NO_3^- in the upper water column to be closer to that of the deep ocean (6.8‰). However, significant ^{15}N-enrichment (up to 15.5‰) of δ^{15}N-NO_3^- in the upper 65 m within Cyclone *Opal* suggests that autotrophic assimilation of NO_3^- was high relative to NO_3^- supply during E-Flux III, implying that the upper water column was relatively isolated.

6. Summary and conclusions

Cyclone *Opal* was a physically mature eddy (4–6 weeks old) when sampled in Spring 2005. The total estimated injection of NO_3^- (213 ± 59 mmol N m^{-2}) was 12 times higher than typically found in this oligotrophic region of the North Pacific subtropical gyre. However, particulate biomass and N isotope compositions were not significantly different when compared to surrounding waters. Estimates of N and C export production inside Cyclone *Opal* were similar to the particle flux in the surrounding waters (Benitez-Nelson et al., 2007; Maiti et al., 2008; Rii et al., 2008). Rapid remineralization of PN within the lower water column (100–150 m) may explain these observations, as implied by other studies within the E-Flux project (Rii et al., 2008; Maiti et al., 2008). A comparison of NO_3^- assimilation and DON accumulation derived in this study implies that 22 ± 15% of the injected NO_3^- accumulates in the DON pool. Indeed, Chen et al. (2008) reported that 87% of organic carbon generated within Cyclone *Opal* accumulated as dissolved organic carbon (DOC) rather than PC.

If we assume that 32 ± 6% of the NO_3^- that was injected remained unassimilated and DON accounted of 22 ± 15% of the injected NO_3^-, then 46 ± 16% of the NO_3^- injected remains undocumented. The large errors associated with the multiple techniques used to estimate the NO_3^- inventory, as well as rates of change of N pools may permit closure of the N budget within Cyclone *Opal*. In addition, excess NO_3^- at 500 m may be indicative of deep remineralization and is sufficient to close the N budget inside the eddy, although there are no supporting data to suggest that remineralization at this depth occurred. Alternatively, lateral transfer of NO_3^- and DON, as well as grazing by microzooplankton may contribute to N mass balance.

This study has provided an intriguing glimpse into how cold-core cyclonic eddies may influence the biogeochemical cycling of N. Yet much more could be learned. In order to understand these complex features, a time-series study tracking the spin up, maturation and degradation of a single eddy would be required in order to appreciate fully their global importance on the N biogeochemistry of oligotrophic systems. In addition, large-scale experiments replicating the injection of sub-surface waters may help us to understand the threshold in nutrients required to initiate a response in the plankton community and a shift in speciation, as well as the temporal dynamics and partitioning of ^{15}N in both the dissolved and particulate pools.

Acknowledgments

We are grateful to the captain and crew of the R/V *Wecoma* for assistance during the E-Flux III cruise. The authors thank Craig Carlson for supplying TDN data. CM thanks the scientists who participated in the E-Flux III cruise for collection of samples, Terri Rust, Marian Westley, Natalie Walsgrove and Brian Popp for assistance in the IRMS laboratory at the University of Hawaii, and Karin Björkman for helpful discussion during the preparation of this manuscript. CM also acknowledges funding from the National Science Foundation and the Gordon and Betty Moore Foundation to DMK. The E-Flux project was supported by NSF Grant OCE-0241645 to CBN.

References

Allen, C.B., Kanda, J., Laws, E.A., 1996. New production and photosynthetic rates within and outside a cyclonic mesoscale eddy in the North Pacific subtropical gyre. Deep-Sea Research I 43 (6), 917–936.

Altabet, M.A., 1988. Variations in nitrogen isotopic composition between sinking and suspended particles: implications for nitrogen cycling and particle transformation in the open ocean. Deep-Sea Research I 35, 535–554.

Altabet, M.A., 1996. Nitrogen and carbon isotopic tracers of the source and transformation of particles in the deep sea. In: Ittekkot, V., Schafer, P., Honjo, S., Depetris, P.J. (Eds.), Particle Flux in the Ocean. Wiley, pp. 155–184.

Altabet, M.A., 2001. Nitrogen isotopic evidence for micronutrient control of fractional NO_3^- utilization in the equatorial Pacific. Limnology and Oceanography 46 (2), 368–380.

Altabet, M.A., Robinson, A.R., Walstad, L.J., 1986. Vertical fluxes of nitrogen in the upper-ocean: a model simulating the alteration of isotopic ratios. Journal of Marine Research 44, 203–225.

Armstrong, F.A.J., Sterns, C.R., Strickland, J.D.H., 1967. The measurement of upwelling and subsequent biological processes by means of the Technicon Autoanalyzer and associated equipment. Deep-Sea Research 14, 381–389.

Benitez-Nelson, C.R., Buesseler, K.O., Karl, D.M., Andrews, J.E., 2001. A time-series study of particulate matter export in the North Pacific Subtropical gyre based on ^{234}Th:^{238}U disequilibrium. Deep-Sea Research I 48, 2595–2611.

Benitez-Nelson, C.R., Bidigare, R.R., Dickey, T., Landry, M.R., Leonard, C.L., Brown, S.L., Nencioli, F., Rii, Y.M., Maiti, K., Becker, J.W., Bibby, T.S., Black, W., Cai, W.-J., Carlson, C., Chen, F., Kuwahara, V.S., Mahaffey, C., McAndrew, P.M., Quay, P.D., Rappé, M., Selph, K.E., Simmons, M.E., Yang, E.J., 2007. Eddy-induced diatom bloom drives increased biogenic silica flux, but inefficient carbon export in the subtropical North Pacific Ocean. Science 316 (5827), 1017–1021.

Bidigare, R.R., Benitez-Nelson, C., Leonard, C.L., Quay, P.D., Parsons, M.L., Foley, D.G., Seki, M.P., 2003. Influence of a cyclonic eddy on microheterotroph biomass and carbon export in the lee of Hawaii. Geophysical Research Letters 30 (6), 1318.

Brown, S.L., Landry, M.R., Selph, K.E., Yang, E.J., Rii, Y.M., Bidigare, R.R., 2008. Diatoms in the desert: Plankton community response to a mesoscale eddy in the subtropical North Pacific. Deep-Sea Research II, this issue [doi:10.1016/j.dsr2.2008.02.012].

Carlson, C.A., Giovannoni, S.J., Hansell, D.A., Goldberg, S.J., Parsons, R., Vergin, K., 2004. Interactions between DOC, microbial processes, and community structure in the mesopelagic zone of the northwestern Sargasso Sea. Limnology and Oceanography 49, 1073–1083.

Carpenter, E.J., Harvey, H.R., Fry, B., Capone, D.G., 1997. Biogeochemical tracers of the marine cyanobacterium *Trichodesmium*. Deep-Sea Research I 44, 27–38.

Casciotti, K.L., Sigman, D.M., Hastings, M.G., Bohlke, J.K., Hilkert, A., 2002. Measurement of the oxygen isotopic composition of nitrate in seawater and freshwater using the denitrifier method. Analytical Chemistry 74, 4905–4912.

Casciotti, K.L., Sigman, D.M., Ward, B.B., 2003. Linking diversity and stable isotope fractionation in ammonium-oxidizing bacteria. Geomicrobiology Journal 20, 353–355.
Chavanne, C., Flament, P., Lumpkin, R., Dousset, B., Bentamy, A., 2002. Scatterometer observations of wind variations by oceanic islands: implications for wind driven ocean circulation. Canadian Journal of Remote Sensing 28 (3), 466–474.
Checkley, D.M., Miller, C.A., 1989. Nitrogen isotope fractionation by oceanic zooplankton. Deep-Sea Research 36, 1449–1456.
Chen, F.-Z., Cai, W.-J., Benitez-Nelson, C.R., Wang, Y., 2007. Sea surface pCO_2–SST relationships across a cold-core cyclonic eddy: implications for understanding regional variability and air–sea gas exchange. Geophysical Research Letters 34, L10603.
Chen, F.-Z, Cai, W.-J, Wang, Y., Rii, Y.M., Bidigare, R.R., Benitez-Nelson, C.R., 2008. The carbon dioxide system and net community production within a cyclonic eddy in the lee of Hawaii. Deep-Sea Research II, this issue [doi:10.1016/j.dsr2.2008.01.011].
Christensen, S., Tiedje, J.M., 1988. Sub-parts-per-billion nitrate method: use of an N_2O producing denitrifier to convert NO_3^- or $^{15}NO_3^-$ to N_2O. Applied Environmental Microbiology 54, 1409–1413.
Cline, J.D., Kaplan, I.R., 1975. Isotopic fractionation of dissolved nitrate during denitrification in the eastern tropical North Pacific Ocean. Marine Chemistry 3, 271–299.
Deutsch, C., Sarmiento, J.L., Sigman, D.M., Gruber, N., Dunne, J.P., 2007. Spatial coupling of nitrogen inputs and losses in the ocean. Nature 445, 163–167.
Dickey, T.D., Nencioli, F., Kuwahara, V.S., Leonard, C., Black, W., Rii, Y.M., Bidigare, R.R., Zhang, Q., 2008. Physical and bio-optical observations of oceanic cyclones west of the island of Hawai'i. Deep-Sea Research II, this issue [doi:10.1016/j.dsr2.2008.01.006].
Dugdale, R.C., Goering, J.J., 1967. Uptake of new and regenerated forms of nitrogen in primary productivity. Limnology and Oceanography 12, 196–206.
Eppley, R.W., Peterson, B.J., 1979. Particulate organic matter flux and planktonic new production in the deep ocean. Nature 282, 677–680.
Falkowski, P.G., Ziemann, D., Kolber, Z., Bienfeng, P.K., 1991. Role of eddy pumping in enhancing primary production in the ocean. Nature 352, 55–58.
Goldman, J.C., McGillicuddy, D.J., 2003. Effect of large marine diatoms growing at low light on episodic new production. Limnology and Oceanography 48, 1176–1182.
Goldthwait, S.A., Steinberg, D.K., 2008. Elevated biomass of mesozooplankton and enhanced fecal pellet flux in cyclonic and mode-water eddies in the Sargasso Sea. Deep-Sea Research II, this issue [doi:10.1016/j.dsr2.2008.01.003].
Hansell, D.A., 2005. Dissolved organic carbon reference material program. EOS 35, 318–319.
Hansell, D.A., Carlson, C.A., 1998. Deep ocean gradients in the concentration of dissolved organic carbon. Nature 395, 263–266.
Hastings, M.G., Sigman, D.M., Lipschultz, F., 2003. Isotopic evidence for source changes of nitrate in rain at Bermuda. Journal of Geophysical Research—Atmospheres 108 (D24), 4790.
Ingalls, A.E., Liu, Z., Lee, C., 2006. Seasonal trends in the pigment and amino acids compositions of sinking particles in biogenic $CaCO_3$ and SiO_2 dominated regions of the Pacific sector of the Southern Ocean along 170°W. Deep-Sea Research I 53, 836–859.
Karl, D.M., Bidigare, R.R., Church, M.J., Dore, J.E., Letelier, R.M., Mahaffey, C., Zehr, J., 2008. The nitrogen cycle in the North Pacific Trades biome: an evolving paradigm. In: Capone, D.G., Carpenter, E.J., Mulholland, M., Bronk, D.A (Eds.), Nitrogen in the Marine Environment, second ed., in press.
Kennedy, H., Robertson, J., 1995. Variations in the isotopic composition of particulate organic carbon in surface waters along an 88°W transect from 67°S to 54°S. Deep-Sea Research II 42 (4/5), 1109–1122.
Knapp, A.N., Sigman, D.M., Lipschultz, F., 2005. N isotopic composition of dissolved organic nitrogen and nitrate at the Bermuda Atlantic Time-series Study site. Global Biogeochemical Cycles 19, GB1018.
Landry, M.R., Brown, S.L., Rii, Y.M., Selph, K.E., Bidigare, R.R., Yang, E.J., Simmons, M.P., 2008. Depth-stratified phytoplankton dynamics in Cyclone *Opal*, a subtropical mesoscale eddy. Deep-Sea Research II, this issue [doi:10.1016/j.dsr2.2008.02.001].
Laws, E.A., 1991. Photosynthetic quotients, new production, and net community production in the open ocean. Deep-Sea Research A 38, 143–147.
Laws, E.A., Popp, B.N., Bidigare, R.R., Kennicutt II, M.C., Macko, S.A., 1995. Dependence of phytoplankton carbon isotopic composition on growth rate and $[CO_2]$aq: theoretical considerations and experimental results. Geochimica Cosmochimica Acta 59, 1131–1138.
Laws, E.A., Falkowski, P.G., Smith Jr., W.O., Ducklow, H., McCarthy, J.J., 2000. Temperature effects on export production in the open ocean. Global Biogeochemical Cycles 14 (4), 1231–1246.
Letelier, R.M., Karl, D.M., Abbott, M.R., Flament, P., Freilich, M., Lukas, R., Strub, R., 2000. Role of late winter mesoscale events in the biogeochemical variability of the upper water column in the North Pacific Subtropical Gyre. Journal of Geophysical Research 105 (C12), 28723.
Lipschultz, F., Bates, N.R., Carlson, C.A., Hansell, D.A., 2002. New production in the Sargasso Sea: history and current status. Global Biogeochemical Cycles 16 (1), 1001.
Liu, K.K., Su, M.-J., Hsueh, C.-R., Gong, G.-C., 1996. The nitrogen isotopic composition of nitrate in the Kuroshiro Water northeast of Taiwan: evidence for nitrogen fixation as a source of isotopically light nitrate. Marine Chemistry 54, 273–292.
Lumpkin, C.F., 1998. Eddies and currents in the Hawaiian Islands. Ph.D. Dissertation, University of Hawaii, 281pp.
Macko, S.A., Fogel, M.L., Hare, P.E., Hoering, T.C., 1987. Isotopic fractionation of nitrogen and carbon in the synthesis of amino acids by microorganisms. Chemical Geology 65, 79–92.
Mahadevan, A., Archer, D., 2000. Modeling the impact of fronts and mesoscale circulation on the nutrient supply and biogeochemistry of the upper ocean. Journal of Geophysical Research 105 (C1), 1209–1226.
Mahaffey, C., Williams, R.G., Wolff, G.A., Anderson, T., 2004. Physical supply of nitrogen to phytoplankton in the Atlantic Ocean. Global Biogeoechemical Cycles 18, GB1034.
Maiti, K., Benitez-Nelson, C.R., Rii, Y.M., Bidigare, R.R., 2008. The influence of a mature cyclonic eddy on particle export in the lee of Hawaii. Deep-Sea Research II, this issue [doi:10.1016/j.dsr2.2008.02.008].
Mariotti, A., Germon, J.C., Huebert, P., Kaiser, P., Letolle, R., Tardieux, A., Tardieux, P., 1981. Experimental determination of nitrogen kinetic isotope fractionation: some principles; illustration for the denitrification and nitrification processes. Plant Soil 62, 413–430.
Martin, A.P., Pondaven, P., 2003. On estimates for the vertical nitrate flux due to eddy-pumping. Journal of Geophysical Research 108 (C11), 3359.
Martin, A.P., Pondaven, P., 2006. New primary production and nitrification in the western subtropical North Atlantic: a modeling study. Global Biogeochemical Cycles 20, GB4014.
McAndrew, P.M., Bidigare, R.R., Karl, D.M., 2008. Primary production and implications for metabolic balance in the Hawaiian lee eddies. Deep-Sea Research II, this issue [doi:10.1016/j.dsr2.2008.01.004].
McGillicuddy, D.J., Robinson, A.R., 1997. Eddy-induced nutrient supply and new production in the Sargasso Sea. Deep-Sea Research I 44, 1427–1450.
McGillicuddy, D.J., Robinson, A.R., Siegel, D.A., Jannasch, H.W., Johnson, R., Dickey, T.D., McNeil, J., Michaels, A.F., Knap, A.H., 1998. Influence of mesoscale eddies on new production in the Sargasso Sea. Nature 394, 263–266.
McGillicuddy, D.J., Johnson, R.J., Siegel, D.A., Michaels, A.F., Bates, N.R., Knap, A.H., 1999. Mesoscale variations of biogeochemical properties in the Sargasso Sea. Journal of Geophysical Research 104 (C6), 13381–13394.
McGillicuddy, D.J., Anderson, L.A., Bates, N.R., Bibby, T., Buesseler, K.O., Carlson, C.A., Davis, C.S., Ewart, C., Falkowski, P.G., Goldthwait, S.A., Hansell, D.A., Jenkins, W.J., Johnson, R., Kosnyrev, V.K., Ledwell, J.R., Li, Q.P., Siegel, D.A., Steinberg, D.K., 2007. Eddy/wind interactions stimulate extraordinary mid-ocean plankton blooms. Science 316, 1021–1026.
McNeil, J.D., Jannasch, H.W., Dickey, T., McGillicuddy, D., Brzezinski, M., Sakamoto, C.M., 1999. New chemical, bio-optical and physical observations of upper ocean response to the passage of a mesoscale eddy off Bermuda. Journal of Geophysical Research 104 (C7), 15537–15548.
Meador, T.B., Aluwihare, L.I., Mahaffey, C., 2007. Isotopic heterogeneity and cycling of organic nitrogen in the oligotrophic ocean. Limnology and Oceanography 52, 934–947.
Nencioli, F., Kuwahara, V.S., Dickey, T.D., Rii, Y.M., Bidigare, R.R., 2008. Physical dynamics and biological implications of a mesoscale eddy in the lee of Hawai'i: Cyclone *Opal* observations during E-Flux III. Deep-Sea Research II, this issue [doi:10.1016/j.dsr2.2008.02.003].
Patzert, W.C., 1969. A study of eddies in Hawaiian waters. Master of Science Thesis, University of Hawaii.
Popp, B.N., Trull, T., Kenig, F., Wakeham, S.G., Rust, T.M., Tilbrook, B., Griffiths, F.N., Wright, S.W., Marchant, H.J., Bidigare, R.R., Laws, E.A., 1999. Controls on the carbon isotopic composition of Southern Ocean phytoplankton. Global Biogeochemical Cycles 13, 827–843.
Rau, G.H., Takahashi, R., Des Marais, D.J., Repeta, D.J., Martin, J.H., 1992. The relationship between delta 13C of organic matter and $[CO_2(aq)]$ in ocean surface water: data from a JGOFS site in the northeast Atlantic Ocean and a model. Geochimica et Cosmochimica Acta 56, 1413–1419.
Redfield, A.C., 1958. The biological control of chemical factors in the environment. American Scientist 46, 205–222.
Rii, Y.M., Brown, S.L., Nencioli, F., Kuwahara, V., Dickey, T., Karl, D.M., Bidigare, R.R., 2008. The transient oasis: Nutrient-phytoplankton dynamics and particle export in Hawaiian lee cyclones. Deep-Sea Research II, this issue [doi:10.1016/j.dsr2.2008.01.013].
Saino, T., Hattori, A., 1987. Geographical variation for the water column distribution of suspended particulate organic nitrogen and its ^{15}N natural abundance in the Pacific and its marginal seas. Deep-Sea Research 34, 807–827.
Sakamoto, C.M., Karl, D.M., Jannasch, H.W., Bidigare, R.R., Letelier, R.M., Walz, P.M., Ryan, J.P., Polito, P.S., Johnson, K.S., 2004. Influence of Rossby waves on nutrient dynamics and the plankton community structure in the North Pacific subtropical gyre. Journal of Geophysical Research 109 (C05032).
Seki, M.P., Polovina, J.J., Brainard, R.E., Bidigare, R.R., Leonard, C.L., Foley, D., 2001. Biological enhancement at cyclonic eddies tracked with GOES thermal imagery in Hawaiian waters. Geophysical Research Letters 28 (8), 1583–1586.
Siegel, D.A., 2001. Oceanography—the Rossby rototiller. Nature 409, 576–577.
Sigman, D.M., Casciotti, K.L., 2001. Nitrogen isotopes in the Ocean. In: Steele, J.H., Turekian, K.K., Thorpe, S.A. (Eds.), Encyclopedia of Ocean Sciences. Academic Press, London, p. 2449.
Sigman, D.M., Casciotti, K.L., Andreani, M., Barford, C., Galanter, M., Bohlke, J.K., 2001. A bacterial method for the nitrogen isotopic analysis of nitrate in seawater and freshwater. Analytical Chemistry 73, 4145–4153.
Sigman, D.M., Granger, J., DiFiore, P., Lehmann, M.F., Geen, A.V., Ho, R., Cane, G., 2005. Coupled nitrogen and oxygen isotope measurements of nitrate along the eastern North Pacific margin. Global Biogeochemical Cycles 19, GB4022.

Strutton, P.G., Ryan, J.P., Chavez, F.P., 2001. Enhanced chlorophyll associated with tropical instability waves in the equatorial Pacific. Geophysical Research Letters 28 (10), 2005–2008.

Sutka, R.L., Ostrom, N.E., Ostrom, P.H., Phanikumar, M.S., 2004. Stable nitrogen isotope dynamics of dissolved nitrate in a transect from the North Pacific Subtropical Gyre to the Eastern Tropical North Pacific. Geochemica et Cosmochimica Acta 68, 517–527.

Sweeney, E.N., McGillicuddy, D.J., Buesseler, K.O., 2003. Biogeochemical impacts due to mesoscale eddy activity in the Sargasso Sea as measured at the Bermuda Atlantic Time-series Study (BATS). Deep-Sea Research II 50, 3017–3039.

Uz, B.M., Yoder, J.A., Osychny, V., 2001. Pumping of nutrients to ocean surface waters by the action of propagating planetary waves. Nature 409, 597–600.

Vaillancourt, R.D., Marra, J., Seki, M.P., Parsons, M.L., Bidigare, R.R., 2003. Impact of a cyclonic eddy field on phytoplankton community structure and photosynthetic competency in the subtropical North Pacific Ocean. Deep-Sea Research I 50, 829–847.

Verdeny, E., Masqué, P., Maiti, K., Garcia-Orellana, J., Bruach, J.M., Mahaffey, C., Benitez-Nelson, C.R., 2008. Particle export within cyclonic Hawaiian lee eddies derived from ^{210}Pb–^{210}Po disequilibrium. Deep-Sea Research II, this issue [doi:10.1016/j.dsr2.2008.02.009].

Wada, E., 1980. Nitrogen isotope fractionation and its significance in biogeochemical processes occurring in marine environments. In: Goldberg, E.D., Saruhashi, K., Horibe, Y. (Eds.), Isotope Marine Chemistry. Uchida-Rokakuho, Tokyo, pp. 375–398.

Wada, E., Hattori, A., 1976. Natural abundance of 15N in particulate organic matter in the North Pacific Ocean. Geochimica et Cosmichimica Acta 40, 249–251.

Waser, N.A.D., Harrison, P.J., Nielson, B., Calvert, S.E., Turpin, D.H., 1998. Nitrogen isotope fractionation during the uptake and assimilation of nitrate, nitrite, ammonium, and urea by a marine diatom. Limnology and Oceanography 43, 215–224.

Waser, N.A.D., Harrison, W.G., Head, E.J.H., Nielsen, B., Lutz, V.A., Calvert, S.E., 2000. Geographic variations in the nitrogen isotope composition of surface particulate nitrogen and new production across the North Atlantic Ocean. Deep-Sea Research I 47, 1207–1226.